JOURNAL OF GEOPHYSICAL RESEARCH, VOL. 112, B02101, doi:10.1029/2006JB004488, 2007

New Tertiary paleomagnetic poles from Mongolia and Siberia at 40, 30, 20, and 13 Ma: Clues on the inclination shallowing problem in central Asia

Fatim Hankard,[1] Jean-Pascal Cogné,[1] Vadim A. Kravchinsky,[1,2] Laurent Carporzen,[1] Amgalan Bayasgalan,[3] and Purevdorj Lkhagvadorj[3]

Received 5 May 2006; revised 6 September 2006; accepted 27 September 2006; published 1 February 2007.

[1] We report results of a paleomagnetic study of 490 cores from 59 sites, corresponding to 52 distinct basaltic flows from Mongolia and Siberia: Khaton Sudal (39.4 Ma, 44.5°N/101.4°E), Taatsyn Gol (1, 31.5 Ma, 45.4°N/101.3°E; 2, 28.0 Ma, 45.5°N/101.1°E), Ust Bokson (19.9 Ma, 52.1°N/100.3°E), and Taatsyn Gol (3, 12.7 Ma, 45.5°N/101.0°E). Stepwise thermal and alternating field demagnetizations isolated a stable high-temperature component (HTC) of magnetization in most specimens, which we interpret as the primary magnetization of these basaltic lava flows. The four corresponding paleopoles appear consistent with coeval paleopoles from other Asian effusive formations. However, except for the 12.7 Ma paleopole, the paleopoles are systematically far-sided from the European apparent polar wander path (APWP) with respect to site locations, corresponding to anomalously shallow inclinations in Tertiary Asian effusive formations. In the hypothesis of a dipolar magnetic field in the Tertiary, this indicates a ~1000–1500 km position of the Siberia craton and Amuria block farther south than expected at 40 and 30 Ma. Tectonically, this interpretation implies decoupling and relative rotations between the western and eastern parts of Eurasia between the Cretaceous and Present. We show that if Siberia were located more to the south, the ~15°–20° paleolatitude anomaly generally observed in sedimentary formations from central Asia reduces to a more reasonable average value of ~7°, which could result from the superimposition of shallowing mechanisms due to sedimentary processes and northward motion of Asian blocks under the effect of ongoing penetration of India into Eurasia in the Tertiary.

Citation: Hankard, F., J.-P. Cogné, V. A. Kravchinsky, L. Carporzen, A. Bayasgalan, and P. Lkhagvadorj (2007), New Tertiary paleomagnetic poles from Mongolia and Siberia at 40, 30, 20, and 13 Ma: Clues on the inclination shallowing problem in central Asia, *J. Geophys. Res.*, *112*, B02101, doi:10.1029/2006JB004488.

1. Introduction

[2] Cretaceous paleoreconstructions of the Asian continent prior to the collision of India [e.g., *Enkin et al.*, 1992; *Chen et al.*, 1993b; *Halim et al.*, 1998b] are primarily based on paleomagnetic data acquired in the different blocks that compose the Asian mosaic. These data reveal that paleomagnetic inclinations within central Asian and Tibetan blocks (e.g., Jungar, Tarim, Qaidam, Kunlun, Qiangtang, and Lhasa blocks) are shallower than the inclinations deduced from the reference apparent polar wander path (APWP) of Eurasia [*Besse and Courtillot*, 1991, 2002]. In contrast, inclinations are generally consistent with the more eastern blocks of north China (NCB) [*Zhao et al.*, 1990; *Zheng et al.*, 1991; *Ma et al.*, 1993; *Sun et al.*, 2006a], south China (SCB) [*Kent et al.*, 1987; *Zhu and Hao*, 1988; *Enkin et al.*, 1991a, 1991b; *Gilder et al.*, 1993; *Morinaga and Liu*, 2004], Korea [*Lee et al.*, 1987], Sikhote Alin [*Otofuji et al.*, 1995, 2003] and Amuria [*Pruner*, 1992; *Cogné et al.*, 2005]. The Cretaceous shallow inclinations of central Asian blocks have been interpreted as resulting from a more southerly location than expected. Subsequently, these mobile blocks have drifted northward with respect to stable Siberia, and undergone relative intracontinental shortening due to the ongoing penetration of India into Eurasia, after its collision at ~50 Ma. The amount of convergence and the distribution of shortening between the various blocks [e.g., *Chen et al.*, 1992] revealed to be consistent with tectonic deformation models for Asia under the effect of a northward convergence of India with Siberia [e.g., *Molnar and Tapponnier*, 1975; *Tapponnier and Molnar*, 1979].

[3] However, paleomagnetic data obtained on Tertiary formations from central Asia are unexpectedly inconsistent with this picture. Tertiary paleomagnetic inclinations are, as for the Cretaceous, shallower than those predicted from the

[1]Laboratoire de Paléomagnétisme, Institut de Physique du Globe de Paris et Université Paris 7, Paris, France.
[2]Now at Physics Department, University of Alberta, Edmonton, Alberta, Canada.
[3]School of Geology, Mongolian University of Science and Technology, Ulaanbaatar, Mongolia.

0148-0227/07/2006JB004488$09.00

European APWP, but the amount of northward drift of blocks and intracontinental shortening deduced from these shallow inclinations are apparently at least twice as large as the amount deduced from Cretaceous data. This leads to the following unacceptable and undocumented paleogeographic interpretations [*Cogné et al.*, 1999]: (1) ~1000 km of north-south extension is required between Siberia and central Asia (e.g., Tarim) from the Cretaceous to ~50 Ma, and (2) intracontinental shortening between the Tarim block and Siberia (within Amuria block) would be larger than 2000 km since 30–50 Ma. This defines the Inclination Anomaly in central Asia.

[4] Several mechanisms have been proposed to explain this anomaly [*Huang and Opdyke*, 1992; *Gilder et al.*, 1993; *Thomas et al.*, 1993; *Westphal*, 1993; *Cogné et al.*, 1999; *Si and Van der Voo*, 2001; *Van der Voo and Torsvik*, 2001; *Tauxe*, 2005]. Synsedimentation and compaction-induced shallowing of magnetization were invoked because almost all paleomagnetic studies were undertaken on sedimentary rocks (red beds) [*Gilder et al.*, 2001; *Tan et al.*, 2003; *Narumoto et al.*, 2006]. Meanwhile, *Chauvin et al.* [1996] demonstrated that for the Tertiary, the inclination-shallowing anomaly amplitude progressively increases from the Atlantic Ocean to central Asia, independently of rock type, and concluded that there was a local magnetic field anomaly at the scale of Eurasia. A global anomaly in the dipole field geometry or the persistence of long-lasting nondipole field terms (quadrupole g_2^0 and/or octupole g_3^0) during the Tertiary was also presented as a possible cause [*Si and Van der Voo*, 2001; *Van der Voo and Torsvik*, 2001]. Nevertheless, *Torcq* [1997] and *Besse and Courtillot* [2002] advocated that the earth's geomagnetic field is close to that of a dipole during the Cretaceous and Tertiary. Even though evidence for a far-sided effect exists for the Tertiary, it induces a maximum error of 2° in latitude corresponding to a maximum inclination error of about 4° at midlatitudes. Detailed studies of the secular variation during the last 5 m.y. also show that the quadrupole contribution to the total magnetic field does not exceed 3–5% [e.g., *Quidelleur et al.*, 1994]. *Cogné et al.* [1999] proposed two other possible causes of Tertiary low inclination: (1) poor constraints on the age of the continental red beds assumed to be of Cenozoic age in Asia, and (2) a poorly constrained paleogeography in central Asia. Assuming that western Eurasia was indeed firmly attached to Europe but that the eastern part (Siberia) could have been located ~1000 km more to the south than predicted for the Tertiary, they proposed that the whole Eurasia plate might have been nonrigid from the Cretaceous to the Present. This south position of the system was believed to be corroborated by the paleolatitudes of SCB, which, albeit consistent with Siberia in the Cretaceous, also displays too shallow inclinations in the Tertiary [e.g., *Gilder et al.*, 1993; *Zhao et al.*, 1994; *Sun et al.*, 2006b].

[5] In order to understand better this crucial problem of shallow inclinations, and in an attempt to define the Cenozoic paleoposition of stable Siberia, we undertook a series of paleomagnetic studies of Cenozoic effusive formations from Mongolia (Amuria block) and south Siberia. Accounting for the various possible causes for inclination shallowing, as cited above, the choice of these formations was guided by the need to (1) get well-dated paleomagnetic data, (2) avoid sedimentary inclination shallowing effects such as compaction, and (3) be located in the northernmost parts of the system, as close to Siberia as possible, in order to avoid India indentation effects. Because the Amuria block was accreted to Siberia by the end of the Jurassic [*Kravchinsky et al.*, 2002; *Cogné et al.*, 2005] and has probably not moved significantly northward with respect to Siberia since then, the Mongolian basalts appear well located to characterize the stable part of the system in the Cenozoic. We report here new paleomagnetic data obtained from four localities of Tertiary (12.7, 28.0, 31.5, and 39.4 Ma) basaltic formations from Mongolia and one (19.9 Ma) from Siberia (Figure 1).

2. Geology, Dating, and Sampling

[6] The Cenozoic volcanic activity in Mongolia is largely confined to longitudinal bands stretching approximately from 94°E to 104°E and from 112°E to 116°E [*Kepezhinskas*, 1979; *Whitford-Stark*, 1987; *Windley and Allen*, 1993; *Yarmolyuk et al.*, 1995; *Barry and Kent*, 1998; *Höck et al.*, 1999], within the Hangai region (Figure 1). Described as "domed" since the Oligocene, the Hangai region is a mountainous area covering more than 200,000 km^2 with numerous flat-topped peaks over 3000 m [*Windley and Allen*, 1993; *Cunningham*, 2001]. This region represents an important kinematic link between the Baikal rift province to the north and the Altai transpressional ranges to the south and west [*Cunningham*, 2001]. Several authors reported that the chemical composition of the basaltic flows from Hangai varies from alkaline to subalkaline (trachybasalt, basalt andesitic, trachy-andesite, tephrite basanites, and their differentiates) [*Whitford-Stark*, 1987; *Kovalenko et al.*, 1997; *Barry and Kent*, 1998; *Barry et al.*, 2003].

[7] Sampling of these basaltic rocks was undertaken during two field trips in the summers of 1999 and 2004, in Mongolia and Siberia. A summary of sampled locations is given in Table 1 (from the oldest to the youngest flows) and in Figure 1. Several sites were sampled for each location. Eight to ten 2.5-cm-diameter cores were drilled at each site using a gasoline-powered drill and oriented in situ using magnetic, and when possible, Sun compasses in order to check and correct for local magnetic field declination (Table 1). When solar readings could not be obtained due to shadows or cloudy weather, we generally used International Geomagnetic Reference Field (IGRF) models to correct for local declination. An exception to this procedure was adopted for Ust-Bokson sites where magnetic declinations measured in the field were much higher than those expected from IGRF (Table 1). Notwithstanding the origin of this discrepancy, which does not seem to be linked to an anomalously high magnetization intensity as reported below, we used the average magnetic declination we measured in the field (Table 1), to correct the cores' magnetic azimuths.

[8] In this paper, we present the paleomagnetic results we obtained at five localities of Cenozoic basaltic flows (Figure 1 and Table 1). We sampled three of these localities at Taatsyn Gol (the Valley of Lakes) in the Gobi Desert of Mongolia. A detailed geological and geochronological study allowed *Höck et al.* [1999] to distinguish three units in this area. On the basis of $^{40}Ar/^{39}Ar$ dating, these authors suggest three main episodes of flow emplacements:

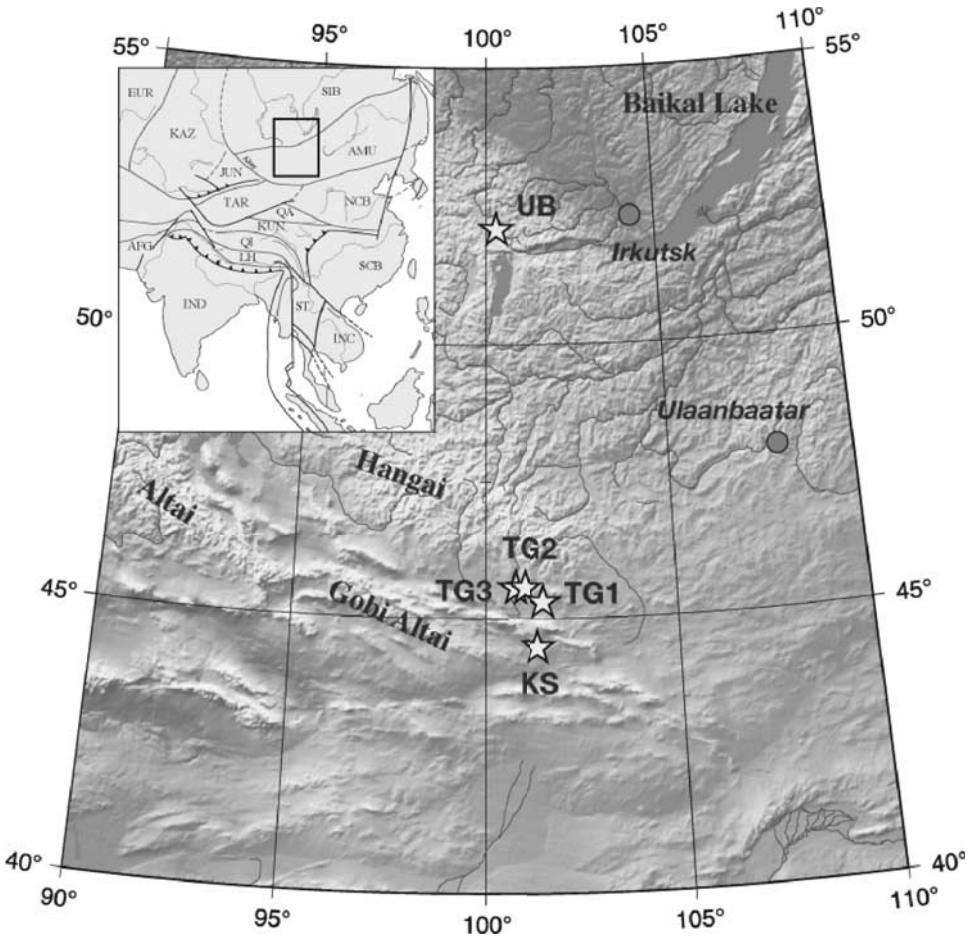

Figure 1. Simplified topographic map showing Tertiary sampling localities (stars) in Mongolia and Siberia (UB, Ust Bokson; KS, Khaton-Sudal; TG, Taatsyn Gol 1, Taatsyn Gol 2, Taatsyn Gol 3); large dots, towns. Inset is a situation map of Figure 1 in Asia, with main blocks indicated (AMU, Amuria; AFG, Afghanistan; EUR, Eurasia main plate; INC, Indochina; IND, India; JUN, Junggar; KAZ, Khazakhstan; KUN, Kunlun; LH, Lhasa; NCB, North China Block; QA, Qaidam; QI, Qiangtang; SCB, South China Block; SIB, Siberia; ST, Shantaï; TAR, Tarim).

(1) basalt I (Taatsyn Gol 1 or TG1, hereafter) provided ages ranging from 30.4 to 32.1 Ma based on 16 independent samples with 1σ standard deviations ranging from 0.3 to 0.8 (average 31.5 ± 0.7 Ma); (2) basalt II (Taatsyn Gol 2 or TG2) based on six samples provided ages ranging from 27.0 to 29.0 Ma with 1σ ranging from 0.4 to 0.9 (average 28.0 ± 0.8 Ma); and (3) basalt III (Taatsyn Gol 3 or TG3) based on nine samples was dated at 12.2 to 13.2 Ma with 1σ ranging from 0.2 to 0.7 (average 12.7 ± 0.6 Ma). Accounting for their detailed mapping of dated outcrops [*Höck et al.*, 1999], we could sample these three areas. We also sampled an older volcanic edifice at Khaton-Sudal (KS) in the Gobi Desert. Although the reported age for this locality is 57.0 ± 0.2 Ma [*Whitford-Stark*, 1987], we have redated this isolated volcanic edifice of neck and flows in the Gobi Desert at two sites using the Gillot-Cassignol K-Ar method [*Cassignol and Gillot*, 1982] at the Geochronological Laboratory of Orsay University. The two ages we obtained are self-consistent (39.1 ± 0.6 and 39.7 ± 0.6 Ma) and provide a mean age of 39.4 ± 0.6 Ma. Because we do not have any information on methods used in the previously reported determination [*Whitford-Stark*, 1987], we rely, herein, on our own age determination. Finally, we sampled a series of basaltic flows in the southeastern part of the Sayan Mountains, south Siberia, on both sides the Oka River, near Ust-Bokson village. *Rasskazov et al.* [2000] dated the two main flow outcrops of the Ust-Bokson location using $^{40}Ar/^{39}Ar$ method at 19.9 ± 0.2 Ma (west of the Oka River; sites 60 to 69 in Table 2) and 19.8 ± 0.2 Ma (east of the Oka River; sites 70 to 73 in Table 2) thus providing a mean location age of 19.9 ± 0.4 Ma.

[9] Finally, because all the Cenozoic flows sampled in this study are flat-lying (e.g., TG1 and UB), and/or underlain by flat-lying sediments (TG1 and TG2), all field measured flow dips (always less than 10° as in TG3) have been interpreted as due to emplacement. Therefore, in the following, no tilt test is applied to paleomagnetic vectors, and all directions are given as in situ.

3. Paleomagnetic Analysis

[10] Minicores, 2.5 cm diameter, were cut in the laboratory into 2.2-cm-long specimens. Magnetic measurements and demagnetization procedures were performed in the

Table 1. Summary of Paleomagnetic Sampling of Cenozoic Basalts From Mongolia and South Siberia[a]

Locality	Location	Lat/Lon	Age	Method	Reference	Sites ID	N/n	Nf	Dec	D_{IGRF}
KS, Khaton-Sudal	Gobi Desert	44.5°N/101.4°E	39.4 ± 0.6	K-Ar	this study	87–94	8/68	8	−1.7° ± 1.6°	−1.4°
TG1, Taatsyn Gol 1	Gobi Desert	45.4°N/101.3°E		$^{40}Ar/^{39}Ar$	*Höck et al.* [1999]	1–3; 20–24; 74–86	21/173	19	−0.7° ± 1.8°	−0.9°
			31.5 ± 0.7							
TG2, Taatsyn Gol 2	Gobi Desert	45.5°N/101.1°E		$^{40}Ar/^{39}Ar$	*Höck et al.* [1999]	12–19	8/70	8	1.2° ± 3.7°	−0.9°
			28.0 ± 0.8							
UB, Ust Bokson	South Siberia	52.1°N/100.3°E		$^{40}Ar/^{39}Ar$	*Rasskazov et al.* [2000]	60–73	14/114	9	21.9° ± 3.0°	−0.1°
			19.9 ± 0.2							
TG3, Taatsyn Gol 3	Gobi Desert	45.5°N/101.0°E		$^{40}Ar/^{39}Ar$	*Höck et al.* [1999]	4–11	8/65	8	−1.1° ± 2.0°	−0.8°
			12.7 ± 0.6							

[a]Lat/Long, average latitude and longitude of the sampling sites (°N/°E); N/n, number of sites/number of cores; Nf, Number of independent flows; Dec, local magnetic field declination computed after magnetic and sun compasses readings; D_{IGRF}, local magnetic field declination computed for the summer 1999 and 2004, after the IGRF coefficients of 1995 and 2000 and their time derivatives.

magnetically shielded room of the paleomagnetic laboratory of the Institut de Physique du Globe de Paris (IPGP) and Paris 7 University at Paris and St. Maur. Remanent magnetization measurements were carried out using Agico JR5 and JR6 spinner magnetometers.

3.1. Magnetic Mineralogy

[11] In order to identify the magnetic mineralogy, isothermal remanent magnetization (IRM) acquisitions were measured on at least one selected specimen per site. Hysteresis loops were determined on a few specimens, using a laboratory-built translation inductometer. Finally, unblocking/blocking temperatures, determined from thermomagnetic susceptibility curves, were measured with Agico KLY 2 and 3 Kappabridge susceptibility meters equipped with CS-2 and -3 furnaces. Experiments were done in both air and argon.

[12] Results of these experiments are shown in Figures 2 to 6, for one representative specimen of each formation. They generally reveal a simple behavior characterized by a low coercivity of 0.3–0.4 T obvious in either IRM acquisition curves (Figures 3c, 4c, 5c, and 6c) or hysteresis loops (Figures 2c, 3d, 4d, 5d, and 6d). Although the susceptibility versus temperature curves are generally not reversible, probably due to heating induced alterations, they show a sharp drop of the susceptibility at about 560–580°C in all sites (Figures 3e, 4e, 5e, and 6e) except for Khaton Sudal (Figure 2d). Altogether, we thus conclude that for all these basaltic formations, the magnetic mineralogy is dominated by Fe-rich titanomagnetites. Only the lower Curie point (∼480–500°C) of Khaton Sudal samples (Figure 2d) indicates a larger Ti content of ∼15%. Finally, the Jrs/Js ratios obtained from hysteresis curves range from ∼0.07 in Khaton Sudal (Figure 2c) to ∼0.5–0.6 in Ust Bokson (Figure 5d) which suggests an average grain size [e.g., *Dunlop*, 2002] within the pseudosingle-domain (PSD) range in most of our samples (Khaton Sudal and Taatsyn Gol 1, 2, and 3), and PSD to single-domain (SD) grain size in Ust Bokson. However, the elevated Jrs/Js observed at Ust Bokson (Figure 5d) may result from the mixture of higher coercivity phase with the Fe-rich titanomagnetites (evidence by the wasp-waisted loop). The high-coercivity phase is also the likely candidate being altered upon heating to higher susceptibilities phase resulting in an order of magnitude increase in room temperature susceptibility after full heating/cooling cycle.

3.2. Demagnetizations

[13] Most specimens were thermally demagnetized over 19 temperature steps up to 590–600°C within a nearly zero field laboratory built furnace at IPGP. Alternating field (AF) demagnetization was conducted on a few samples over 14 steps up to 100 mT. During thermal demagnetization, sample orientation was successively inverted about the *z* axis in order to detect any systematic magnetization that could have resulted from the small ∼10 nT residual magnetic field in the furnace.

[14] Demagnetization results were plotted as orthogonal vectors diagrams [*Zijderveld*, 1967] and also as equal-area projections. Both paleomagnetic directions were determined using principal component analysis [*Kirshvink*, 1980] or remagnetization great circles [*Halls*, 1978; *McFadden and*

Table 2. Site-Mean Paleomagnetic Directions for the High-Temperature Component of Tertiary Effusives From Mongolia and South Siberia[a]

Sites	Type	n/N	Dg, deg	Ig, deg	k	α_{95}, deg
Khaton Sudal (KS), 39.4 ± 0.6 Ma, 44.5°N/101.4°E						
87	HT	9/9	193.1	−64.1	37.1	8.6
88	HT + GC	9/9	196.5	−58.2	969.1	1.7
89	HT	9/9	214.9	−59.2	149.5	4.2
90	HT	9/9	218.5	−53.3	351.5	2.8
91	HT	6/7	199.6	−48.8	65.5	8.3
92[b]	GCm	8/9	62.2	−28.1		
93	HT	8/8	199	−68.0	293.5	3.2
94	HT	7/8	193.9	−53.0	360.3	3.2
Average KS	-	8/8	202.9	−57.9	93.5	5.8
Taatsyn Gol 1 (TG1), 31.5 ± 0.7 Ma, 45.4°N/101.3°E						
01	HT	6/7	189.0	−55.0	204.4	4.7
02	HT + GC	7/7	180.7	−43.8	139.2	5.4
03	HT	6/7	191.0	−52.1	111.2	6.4
20	HT	7/7	176.2	−57.8	282.4	3.6
21	HT	8/8	177.1	−52.4	629.3	2.2
22	HT	6/7	179.5	−54.8	378.0	3.5
23	HT	6/7	161.9	−58.4	117.0	6.2
24	HT	7/7	178.3	−54.3	605.7	2.5
74[c]	HT	4/9	113.8	−7.1	67.6	11.3
75	HT	9/9	185.8	−46.9	61.7	6.6
76–78	HT + GC	16/19	177.5	−53.7	44.5	5.6
77–79	HT	18/20	181.3	−50.4	110.5	3.3
80	HT	9/9	181.1	−51.6	27.8	9.9
81	HT	8/9	185.6	−52.1	150.1	4.5
82	HT + GC	10/10	177.8	−75.8	55.1	6.7
83	HT + GC	9/9	179.3	−41.9	167.7	4.0
84	HT	9/11	179.5	−55.8	88.2	5.5
85	HT + GC	9/9	168.1	−65.9	97.2	5.3
86	HT	5/9	195.3	−41.2	138.9	6.5
Average TG1	-	18/19	1.0	53.8	75.5	4.0
Taatsyn Gol 2 (TG2), 28.0 ± 0.8 Ma, 45.5°N/101.1°E						
12	HT	7/7	355.0	56.7	105.1	5.9
13	HT	6/7	2.0	61.7	156.9	5.4
14	HT	7/7	6.0	61.0	638.7	2.4
15	HT	7/7	7.5	71.5	287.4	3.6
16	HT	7/7	2.3	64.8	497.3	2.7
17	HT	7/7	358.2	66.7	342.8	3.3
18	HT	6/6	353.0	61.7	225.6	4.5
19	HT	7/8	7.3	64.4	422.3	2.9
Average TG2	-	8/8	1.0	63.7	257.3	3.5
Average TG1-2, 29.8 ± 1.5 Ma		26/27	1.0	56.8	74.7	3.3
Ust-Bokson (UB), 19.9 ± 0.4 Ma, 52.1°N/100.3°E						
60–61	HT + GC	11/12	29.2	60.1	387.0	2.3
62–63	HT	12/12	39.1	60.4	184.3	3.2
64–65	HT	11/12	41.7	61.5	299.0	2.5
66	HT	6/6	35.4	63.8	192.7	4.8
67	HT	6/6	34.3	61.1	304.3	3.8
68–69	HT	12/12	48.9	59.0	216.2	3.0
70	HT + GC	6/6	186.0	−77.8	615.2	3.1
71–72	HT	12/12	190.9	−75.2	157.7	3.5
73	HT	6/6	181.1	−73.8	170.5	5.1
Average UB	-	9/9	31.7	66.5	70.3	6.2
Taatsyn Gol 3 (TG3), 12.7 ± 0.6 Ma, 45.5°N/101.0°E						
4	HT + GC	7/7	207.1	−53.9	129.3	5.7
5	HT + GC	7/7	199.5	−56.8	339.3	3.4
6	HT + GC	8/9	212.4	−55.0	156.0	5.0
7	HT + GC	8/8	251.1	−67.5	93.2	5.8
8[d]	GCi	6/6	218.4	−77.1	-	12.7
9[c]	HT + GC	8/8	344.8	−80.7	658.7	2.4
10	HT + GC	4/7	183.5	−52.9	98.0	10.8
11	HT	7/7	180.7	−80.1	90.4	6.4
Average TG3	-	7/8	206.6	−64.7	29.5	11.3

[a]HT, high-temperature magnetization component; GC, remagnetization great circle; n/N, number of samples used in the statistics/number of demagnetized specimens; Dg/Ig, declination/inclination in geographic coordinates; k, α_{95}, parameters of Fisher statistics.
[b]Site 92, GCm is the normal to the average great circle; $\alpha_{95x} = 2.6$ and $\alpha_{95y} = 4.3$.
[c]Sites 9 and 74 excluded from the final mean calculations.
[d]Site 8, GCi is the intersection of remagnetization great circles.

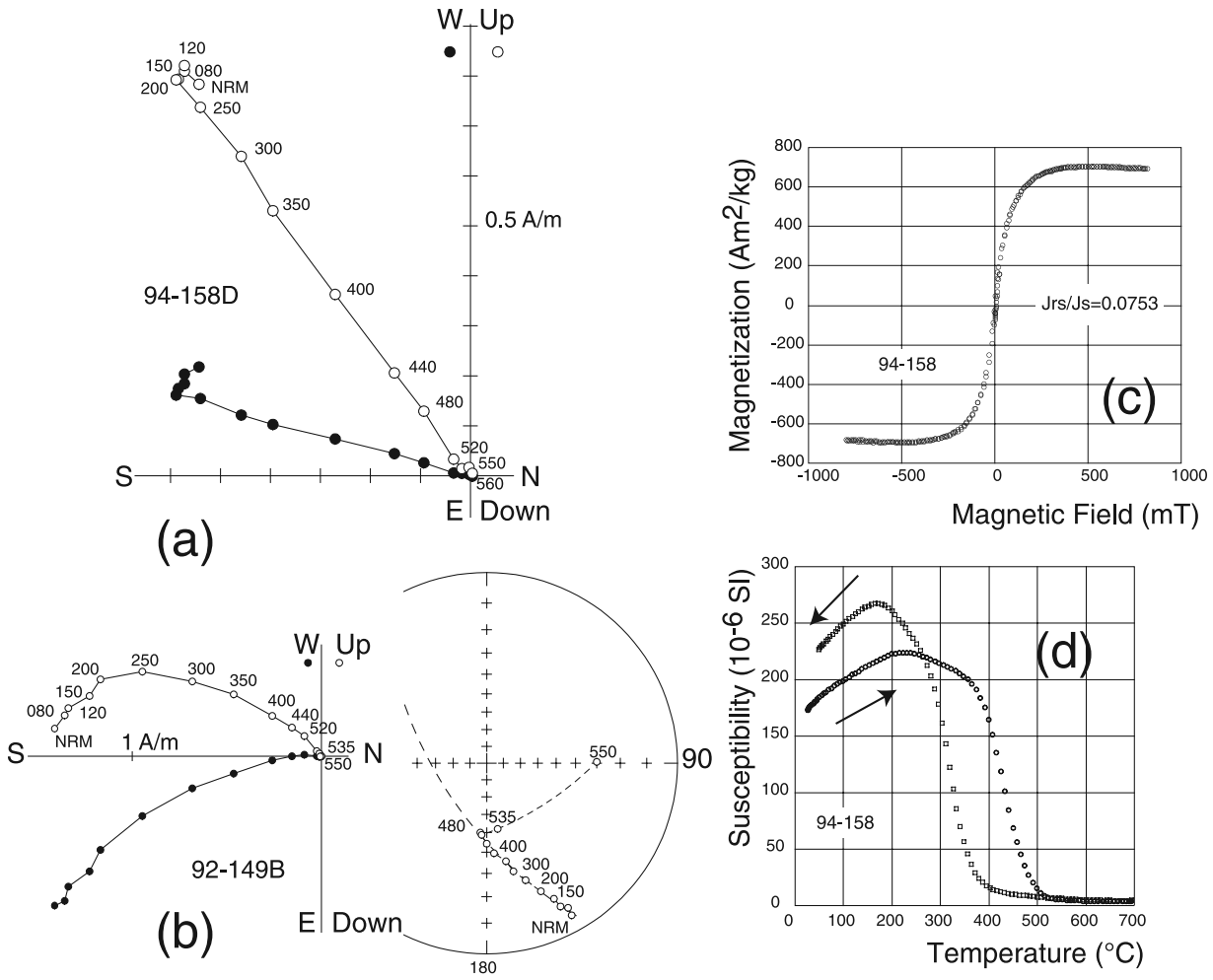

Figure 2. Demagnetizations and rock magnetism experiments on Khaton Sudal (39.4 Ma) specimens. (a) Orthogonal vector plot [*Zijderveld*, 1967] of thermal demagnetization exhibiting a single magnetic component, after removal of a low-temperature component by 200°C; temperatures in °C. (b) Orthogonal vector plot showing overlapping unblocking temperature spectra between two magnetization components, in which case, data are interpreted using the remagnetization great circle method [*McFadden and McElhinny*, 1988], shown on the stereonet to the right. (c) Hysteresis loop after correction of paramagnetic component showing the presence of low-coercivity magnetic mineral; field in mT. (d) Susceptibility curve versus temperature showing an unblocking temperature at ~480–500°C. Temperatures are indicated in °C; arrows indicate heating or cooling. Black (white) symbols in orthogonal vector plots in Figures 2a and 2b indicate projection onto the horizontal (vertical) plane; black (white) symbols in stereonet in Figure 2b indicate downward (upward) pointing vectors.

McElhinny, 1988]. Site-mean directions were calculated using *Fisher* [1953] statistics or using the statistics of *McFadden and McElhinny* [1988] for combined directional data and great circles. All interpretations and data processing were carried out using the PaleoMac software [*Cogné*, 2003] developed at IPGP. In the following, results of demagnetization experiments are detailed in reverse chronological order, from the oldest to the youngest unit.

3.2.1. Khaton Sudal (KS) Locality (39.4 Ma, 44.5°N/101.4°E)

[15] The 68 samples from eight sites collected in Khaton Sudal volcanic edifice have natural remanent magnetization (NRM) intensity between 6.0 and 0.5 A/m with an average value around 2.2 ± 1.5 A/m (n = 68). Almost 45% of the studied specimens displayed only a single high-temperature component (HTC) which trends linearly toward the origin of the vector diagrams in a south and upward direction, and vanishes at 550°C. However, 40% of specimens displayed two magnetization components during progressive thermal and AF demagnetization. A low-temperature magnetization component (LTC) is removed by 200° to 300°C (Figure 2a) and a HTC unblocks at 550°C or 100 mT. In the remaining 15% of the samples, the demagnetization paths display overlapping LTC and HTC unblocking temperature spectra (Figure 2b). Thus demagnetization paths from all specimens from site 92 and one from site 88 aligned along great circle trajectories. For this reason, the site-mean direction of site 88 was computed using the combined average of *McFadden and McElhinny* [1988]. On the other hand, we computed an

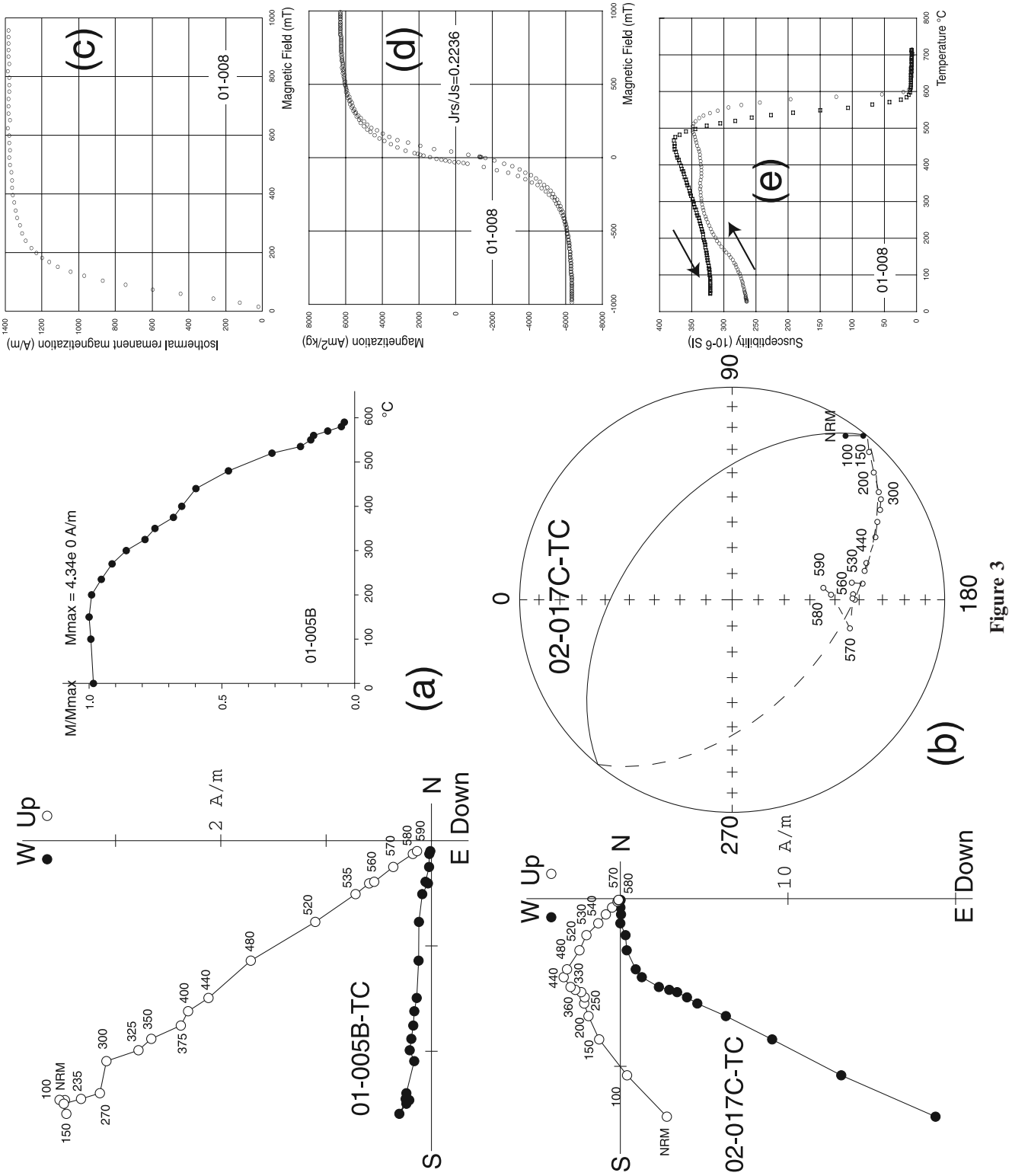
(a)
M/Mmax
Mmax = 4.34e 0 A/m
01-005B
°C
W Up
2 A/m
S
N
E Down
01-005B-TC
NRM
(b)
02-017C-TC
0
90
180
270
10 A/m
(c)
01-008
Isothermal remanent magnetization (A/m)
Magnetic Field (mT)
(d)
Jrs/Js=0.2236
Magnetization (Am2/kg)
(e)
Susceptibility (10-6 SI)
Temperature °C

Figure 3

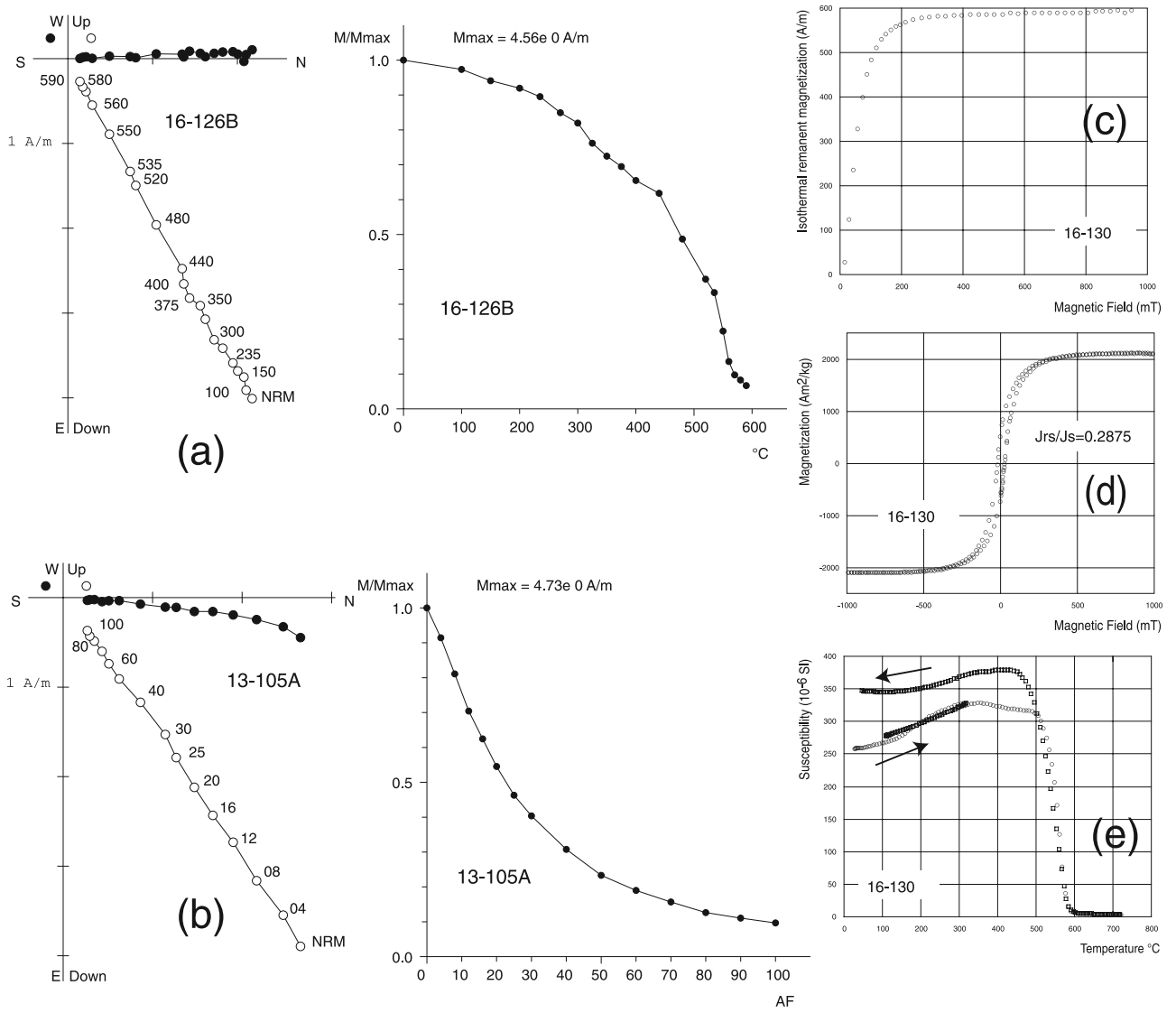

Figure 4. Demagnetizations and rock magnetism experiments on Taatsyn Gol 2 (28.0 Ma) specimens. (a) Orthogonal vector plot [*Zijderveld*, 1967] of thermal demagnetization exhibiting (left) a single magnetic component and (right) magnetization decay curve showing maximum unblocking temperature of ~580°C. (b) Orthogonal projection of (left) alternating field (AF) demagnetization and (right) magnetization decay curve; AF in mT. (c), (d) and (e) Same as in Figure 3. Conventions, symbols, and indications are the same as in Figure 2.

average remagnetization great circle, using the bivariate statistics of *Le Goff* [1990] for site 92.

3.2.2. Taatsyn Gol 1 (TG1) Locality (31.5 Ma, 45.4°N/101.3°E)

[16] At this locality, we distinguish two groups of NRM intensity. The first group, comprising 159 specimens out of 178, displays NRM intensities ranging from 0.003 to 10 A/m, with a mean value of 3.8 ± 2.2 A/m (n = 159). In the second group, 19 specimens exhibit much higher values, varying from 12 to 34 A/m (up to 62 for one specimen), with a mean value of 21.4 ± 12.1 A/m (n = 19). We suspect samples with high NRM intensities to have acquired a

Figure 3. Demagnetizations and rock magnetism experiments on Taatsyn Gol 1 (31.5 Ma) specimens. (a) Orthogonal vector plot [*Zijderveld*, 1967] of thermal demagnetization exhibiting (left) a single magnetic component and (right) magnetization decay curve showing maximum unblocking temperature of ~580°C. (b) Orthogonal projection of thermal demagnetization of (left) a sample showing two partly overlapping components of magnetization and (right) corresponding evolution along a great circle. (c) Isothermal remanent magnetization (IRM) acquisition curve up to 1 T field showing saturation at ~400 mT. (d) Hysteresis loop after correction of paramagnetic component showing the presence of low-coercivity magnetic mineral; field in mT. (e) Susceptibility curve versus temperature showing an unblocking temperature of 580°C. Conventions, symbols, and indications are the same as in Figure 2.

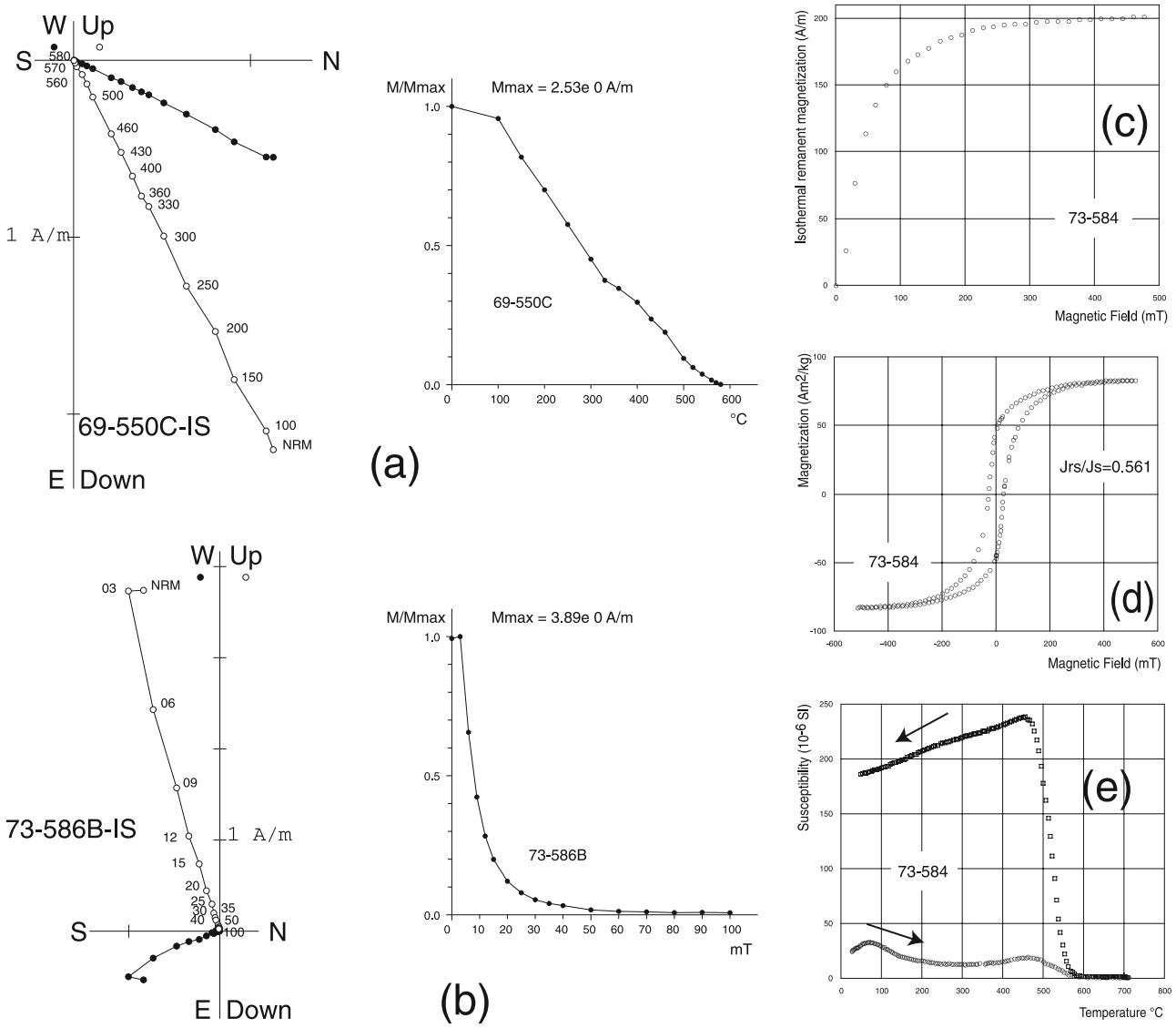

Figure 5. Demagnetizations and rock magnetism experiments on Ust Bokson (19.9 Ma) specimens. (a) to (e) Same as in Figure 4. Conventions, symbols, and indications are the same as in Figure 2.

lightning induced partial isothermal remanent magnetization (IRM). In effect, this IRM was easily removed below 300–330°C and 16 mT during thermal and AF demagnetization processes, respectively. In most specimens, demagnetization analyses yielded a single, south and upward, high-temperature magnetic component (HTC), isolated between 400°C and 590°C and in peak AF fields between 12 mT and 100 mT (Figure 3a). However, in 6 of the 21 sites, the HTC follows a low-temperature component (LTC) which unblocks between room temperature and 300–350°C (Figure 3b). Because of overlapping unblocking spectra, magnetization components could not always be confidently separated. In such cases, we used the remagnetization great circles (Figure 3b), and computed the site-mean directions using *McFadden and McElhinny* [1988] statistics.

3.2.3. Taatsyn Gol 2 (TG2) Locality (28.0 Ma, 45.5°N/101.1°E)

[17] Samples are strongly magnetized with NRM varying from 2.6 to 6.6 A/m with a mean intensity of 5.0 ± 1.6A/m (n = 56). The magnetization behavior upon either thermal (Figure 4a) or AF (Figure 4b) demagnetization is generally simple and exhibits a single component of magnetization, which converges toward the origin of orthogonal plots. This HTC is completely demagnetized by 570–580°C and almost removed at 100 mT. The maximum unblocking temperature together with magnetic mineralogy experiments indicate magnetite as the magnetic carrier of HTC.

3.2.4. Ust Bokson (UB) Locality (19.9 Ma, 52.1°N/100.3°E)

[18] Natural remanent magnetization (NRM) intensity of these basaltic lava flows ranges from 0.5 A/m to 11 A/m with a mean value of 3.4 ± 2.1 A/m (n = 84). Thermal (Figure 5a) and AF (Figure 5b) demagnetizations reveal a single component of magnetization which completely demagnetizes by 570–580°C (Figure 5a) and 60–80 mT (Figure 5b). This magnetization shows a downward north normal direction in sites 60 to 69 from the western side of the Oka River, and an upward south reverse direction

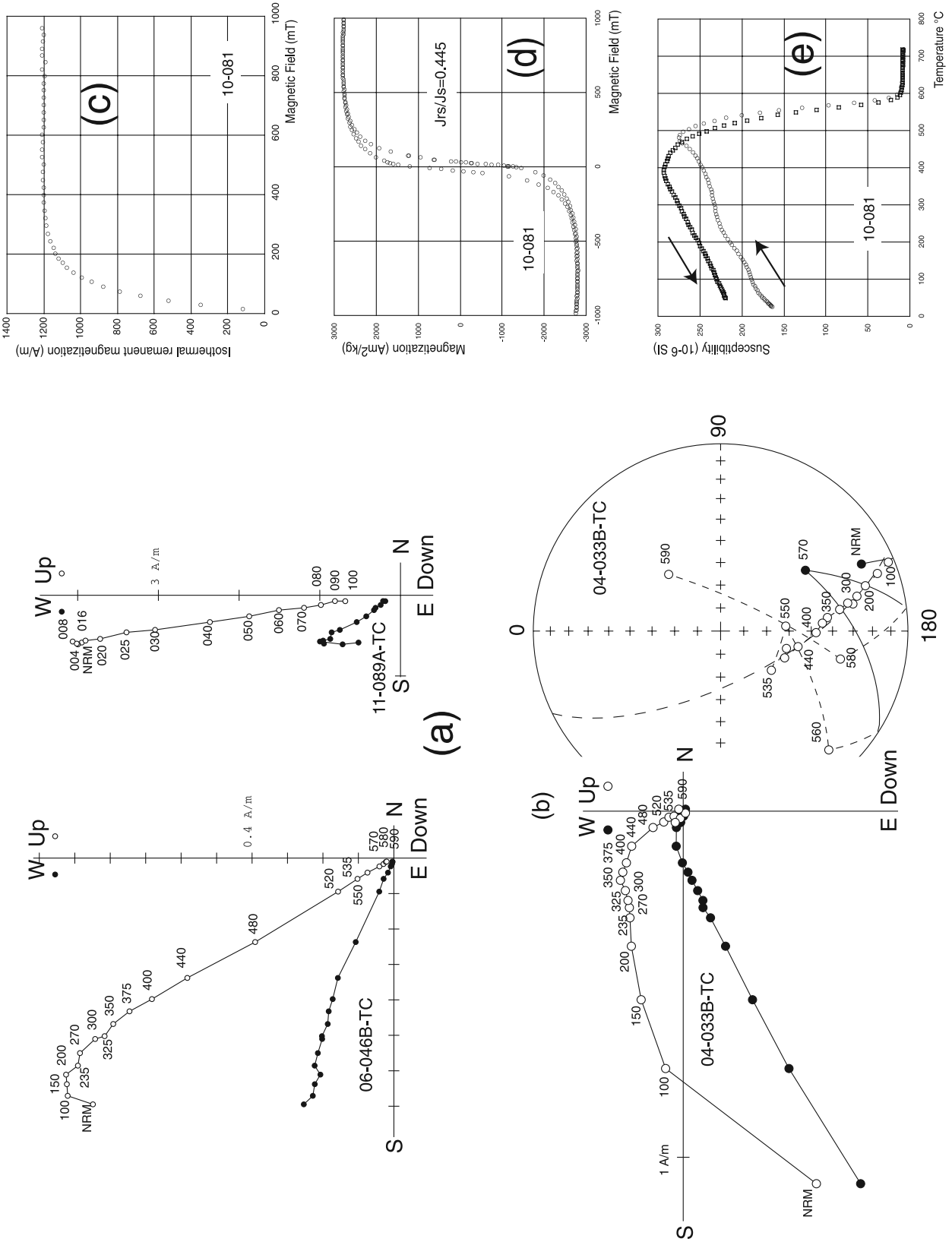
(a)
W Up
0.4 A/m
NRM
100
150
200
235
270
300
325
350
375
400
440
480
520
535
550
570
580
590
S
N
E Down
06-046B-TC
W Up
3 A/m
NRM
004
008
016
020
025
030
040
050
060
070
080
090
100
S
N
E Down
11-089A-TC
(b)
W Up
1 A/m
NRM
100
150
200
235
270
300
325
350
375
400
440
480
520
535
590
S
N
E Down
04-033B-TC
0
90
180
04-033B-TC
NRM
100
200
300
350
400
440
535
550
560
570
580
590
(c)
10-081
Isothermal remanent magnetization (A/m)
Magnetic Field (mT)
(d)
10-081
Jrs/Js=0.445
Magnetization (Am2/kg)
Magnetic Field (mT)
(e)
10-081
Susceptibility (10-6 SI)
Temperature °C

Figure 6

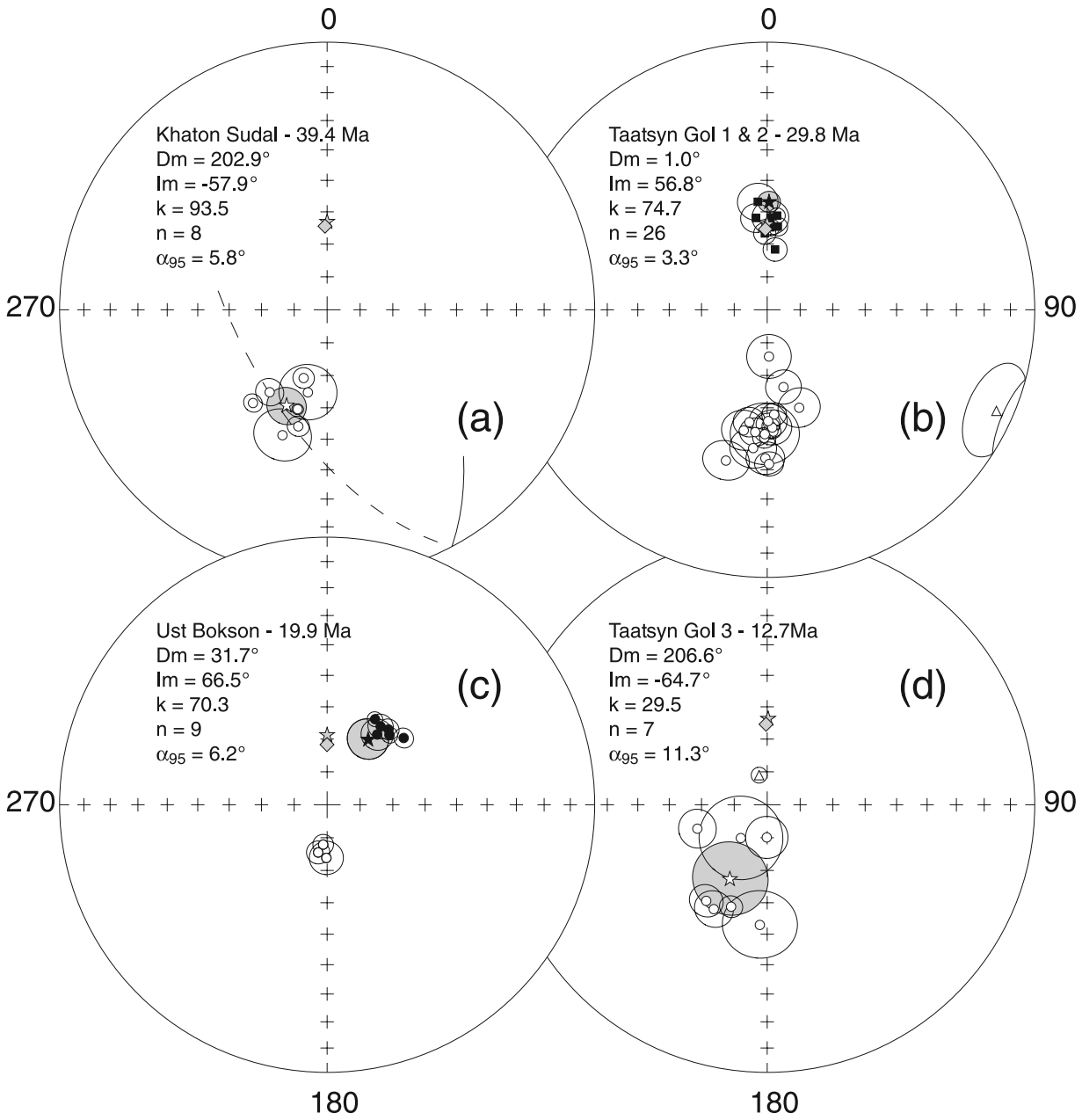

Figure 7. Equal-area projections of HTC flow-mean directions with their α_{95} cones of confidence at (a) Khaton-Sudal, (b) Taatsyn Gol 1 (white dots) and 2 (black squares), (c) Ust Bokson, and (d) Taatsyn Gol 3. Stars with shaded α_{95} areas indicate overall mean HTC; gray stars and diamonds indicate dipole and IGRF field directions, respectively; triangles in Figures 7b and 7d indicate data excluded from the computation of the final mean; solid (open) symbols indicate positive, downward, (negative, upward) inclinations; hatched line in Figure 7a indicates average remagnetization great circle of site 92.

in sites 70 to 73, from the other bank. Only three specimens out of 84 behaved differently, displaying overlapped of unblocking temperature spectra of two components, thus leading to a great circle path of points during demagnetization.

3.2.5. Taatsyn Gol 3 (TG3) Locality (12.7 Ma, 45.5°N/101.0°E)

[19] Natural remanent magnetization (NRM) intensity of these eight basaltic lava flows ranges from 0.04 to 4.80 A/m with a mean value of 1.3 ± 1.0 A/m (n = 59). Generally for

Figure 6. Demagnetizations and rock magnetism experiments on Taatsyn Gol 3 (12.7 Ma) specimens. (a) Orthogonal vector plot [*Zijderveld*, 1967] of (left) thermal and (right) AF demagnetizations showing a high-temperature component (HTC) isolated after ~300°C and ~20 mT. (b) Orthogonal vector plot of thermal demagnetization showing (left) two partly overlapping magnetization components and (right) the resulting great circle evolution of magnetic vectors in stereonet. (c), (d) and (e) Same as in Figure 3. Conventions, symbols, and indications are the same as in Figure 2.

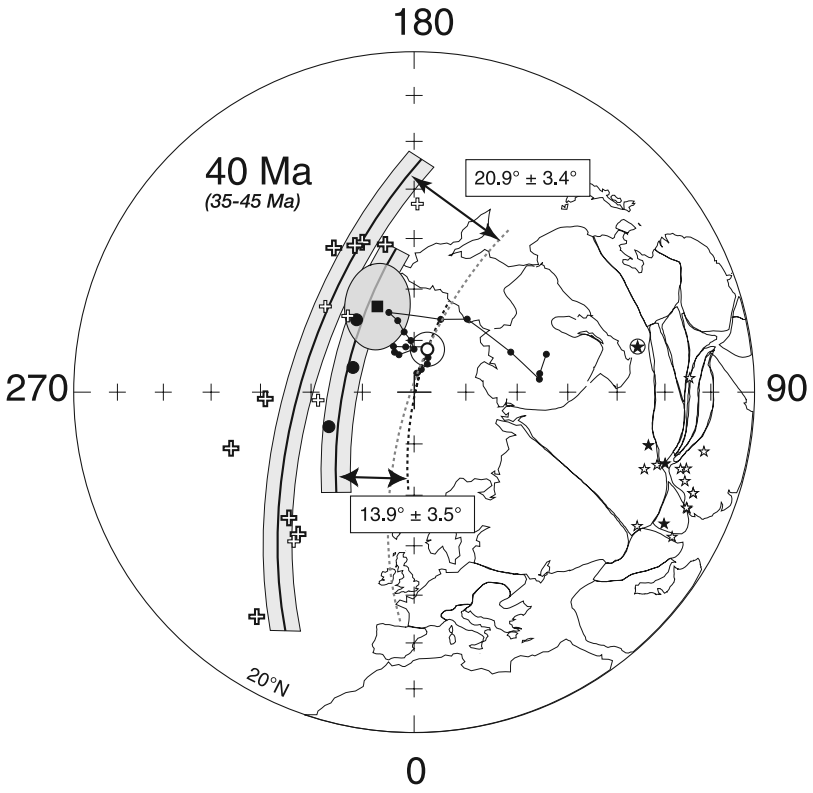

Figure 8. Equal-area projection of the Earth's northern hemisphere limited to the 20°N latitude showing the 39.4 Ma Khaton-Sudal paleopole (black square with shaded dp/dm ellipse of confidence) and selected paleopoles within the 35–45 Ma time period. White plus symbols indicate paleopoles obtained from sedimentary formations (bold white plus, data coming from the India plate); white stars indicate sampling localities in sedimentary formations; black dots indicate paleopoles obtained from effusive formations; black stars indicate sampling localities of effusive formations. Two small circles (black lines with shaded areas of confidence) centered on average site locations are drawn over the populations of sedimentary and effusive paleopoles and compared to small circles (dotted lines) passing through the 40 Ma pole (white dot with A_{95} circle of confidence) of Europe APWP (small joined black dots). Circled black star indicates Khaton-Sudal locality.

most of our samples (52 out of 59 samples), we used both principal component analysis and remagnetization great circle technique to separate the magnetic components. Many of the samples for which principal component analysis was applied possessed two magnetic components. The first, a low-temperature component (LTC) was generally defined between the 300°C and 440°C temperature steps of the thermal treatment or between 8 and 40 mT in AF demagnetization, after removing a recent field or weak viscous magnetization. The second, an upward south high-temperature component (HTC) that does decay toward the origin, was removed between 480°C and 590°C or between 40 and 100 mT (Figure 6a). Concerning the remaining samples, we used the remagnetization great circle technique because demagnetization vector paths aligned on great circles due to an overlap of the LTC and HTC unblocking temperature spectra, (Figure 6b). Therefore, in most cases (except site 11), the site-mean directions of HTC (Table 2) were computed using the mixed average of *McFadden and McElhinny* [1988]. Concerning site 08, magnetic components of all specimens were resolved using only the great circle technique. For this site, because the great circles intersect at a single point, the intersection point was used as the suspected HTC site-mean direction (Table 2). Finally, some samples (particularly from site 10) have been rejected because of their very noisy demagnetization behavior.

4. Paleomagnetic Results and Paleopoles

[20] All the above paleomagnetic analyses and magnetic mineralogy experiments have shown that for most sites sampled, the recovered stable magnetization component is carried by magnetite. Because neither our field observations nor studies by others in the region show any evidence of tectonic tilting since the emplacement of these flows, fold or tilt test could not be performed on the paleomagnetic directions. However, the magnetization in all our samples is carried by a stable, high unblocking temperature and low-coercivity magnetite, and in a number of localities (Khaton Sudal, Taatsyn Gol 1 and 3, a part of Ust Bokson), magnetization appears to be of reverse polarity. We interpret that the HTC identified by thermal and AF demagnetizations is the primary magnetization of the flows. The mean paleomagnetic directions are listed in situ in Table 2 and illustrated on equal-area projections in Figure 7. For each formation, we have computed the means at the flow level as identified in the field, which results in a total of 52 flow-mean directions from 59 sampled sites. More than 69% of

Table 3. Selected Paleopoles From Asia

	Basin/Terrane	Age (Mean)	Site Lat.	Site Long.	Paleopole Lat.	Paleopole Long.	dp/dm (A_{95})	Paleolatitude Observed	Paleolatitude Experimental	ΔPlat	References	Result[a]
					35–45 Ma							
Europe APWP		40.0			81.3	162.4	3.3				*Besse and Courtillot* [2002]	
Sediments												
Tajikistan		36.0	39.4	73.3	53.0	179.0	4.3/7.2	22.4	39.0	−16.6	*Bazhenov et al.* [1978]	4171
India		39.5	33.1	74.3	59.0	202.0	2.0/3.5	11.8	33.0	−21.2	*Klootwijk et al.* [1986]	565
Pakistan		40.0	30.0	70.1	57.7	209.1	2.1/4.2	4.2	29.3	−25.1	*Klootwijk et al.* [1981]	224
Pakistan		40.0	30.0	66.9	55.2	315.3	4.5/8.3	13.2	28.8	−15.6	*Klootwijk et al.* [1981]	234
Pakistan		40.0	30.0	70.1	60.7	191.2	3.1/5.8	12.5	29.3	−16.8	*Klootwijk et al.* [1981]	222
Pakistan		40.0	30.2	67.0	54.0	320.9	2.0/3.6	15.4	29.0	−13.6	*Klootwijk et al.* [1981]	229
Pakistan		40.0	30.2	60.7	52.3	321.1	5.1/9.0	18.1	28.1	−10.0	*Klootwijk et al.* [1981]	231
Pakistan		40.0	30.0	70.1	61.0	272.7	1.6/3.2	2.8	29.3	−26.5	*Klootwijk et al.* [1981]	220
Tibet		41.0	34.6	92.9	70.4	221.0	11.8/20.1	21.4	37.2	−15.8	*Liu et al.* [2003]	8970
Turkmenistan		41.0	38.0	59.0	66.0	226.0	3.0/5.4	14.5	35.5	−21.0	*Mammedov* [1971]	4129
Uzbekistan		44.0	41.7	71.5	71.3	274.8	6.8/11.0	24.2	41.0	−16.8	*Thomas et al.* [1993]	7433
India		44.0	34.3	73.9	35.0	325.0	2.0/4.0	6.0	34.1	−28.1	*Klootwijk et al.* [1986]	568
Pakistan		45.0	32.6	71.8	52.4	287.2	5.4/10.7	0.5	32.1	−31.6	*Haag and Heller* [1991]	6365
India		45.0	30.2	78.4	59.0	199.0	5.5	11.8	30.7	−18.9	*Klootwijk et al.* [1982]	774
Average sediments small circle[b]		41.1 ± 2.5	33.4	71.4								
Effusives												
Kyrgyzstan		38.0	42.4	77.1	77.1	248.5	5.6/8.6	29.6	42.5	−12.9	*Thomas et al.* [1993]	7274
Khaton-Sudal		39.4	44.5	101.4	72.0	202.6	6.3/8.5	38.6	48.2	−9.6	this study	
Afghanistan		39.5	33.3	62.1	72.0	219.0	6.9/12.3	16.5	31.3	−14.8	*Krumsiek* [1976]	2382
Tajikistan		44.0	38.0	74.0	72.0	292.0	5.1/8.4	23.2	37.7	−14.5	*Davydov et al.* [1986]	4175
Average effusives small circle[c]		40.2 ± 2.6	40.4	77.8								
					25–35 Ma							
Europe APWP		30.0			82.8	158.1	3.8				*Besse and Courtillot* [2002]	
Sediments												
Tajikistan	SW Ghissar Range	25.5	38.2	66.3	67.4	237.7	5.9/10.7	15.8	37.6	−21.8	*Chauvin et al.* [1996]	8091
Uzbekistan	Ferghana Basin	27.0	41.3	71.3	62.6	290.8	5.9/10.3	18.6	41.3	−22.7	*Thomas et al.* [1993]	7276
Tajikistan	Peter I Range	27.5	38.8	70.3	66.0	270.0	4.3/7.8	15.9	38.7	−22.8	*Bazhenov et al.* [1978]	4167
Tajikistan	Peter I Range	27.5	38.9	70.9	59.0	319.0	5.1/8.4	22.9	38.9	−16.0	*Bazhenov et al.* [1978]	4169
Tajikistan	Peter I Range	27.5	38.4	70.4	59.0	305.0	7.6/13.5	17.4	38.3	−20.9	*Bazhenov et al.* [1978]	4170
Tajikistan	South Darvaz	27.5	37.7	68.1	43.5	326.0	7.0/12.5	17.5	37.4	−19.9	*Thomas et al.* [1994]	7492
Tajikistan	Peter I Range	27.5	38.0	70.1	37.0	331.0	4.2/7.7	15.7	37.9	−22.2	*Bazhenov et al.* [1978]	4168
Tajikistan	Zaalaisky Range	27.5	39.6	73.3	54.1	181.4	3.8/6.3	22.1	39.9	−17.8	*Bazhenov and Burtman* [1990]	7840
Tajikistan	Khozretishi Range	27.5	37.9	70.2	36.9	330.9	4.1/7.5	15.5	37.8	−22.3	*Bazhenov and Burtman* [1990]	7841
China	Hexi	28.5	40.0	97.7	66.8	256.5	3.9/6.8	18.0	43.2	−25.2	*Dupont-Nivet et al.* [2003]	9169
China	Qaidam Basin	28.5	38.7	92.8	75.1	243.5	4.0/6.4	25.4	41.4	−16.0	*Dupont-Nivet et al.* [2002]	9044
China	Altyn Tagh Range	28.5	38.9	91.4	80.6	243.9	4.8/7.2	30.5	41.4	−10.9	*Dupont-Nivet et al.* [2003]	9167
China	Qaidam Basin	28.5	37.5	95.2	70.8	242.3	7.9/13.5	20.8	40.5	−19.7	*Dupont-Nivet et al.* [2002]	9043
Kyrgyzstan	Northern Tien Shan	28.5	42.4	78.2	73.4	258.2	8.6/13.8	25.8	43.3	−17.5	*Thomas et al.* [1993]	7272
Uzbekistan	Fergana	29.0	41.0	72.0	73.0	259.0	4.4/7.3	24.1	41.1	−17.0	*Yeroshkin* [1973]	4138
Tajikistan	Pamirs	29.0	38.8	70.4	66.1	296.0	4.3/7.3	20.6	38.7	−18.1	*Bazhenov and Burtman* [1990]	7838
China	Tibetan Plateau	30.5	35.0	93.0	57.4	188.8	7.7/12.7	26.0	37.8	−11.8	*Liu et al.* [2003]	8969
Average sediments small circle[d]		28.0 ± 1.1	39.4	77.4								
Effusives												
Mongolia	Khan-Uul	29.5	43.5	104.5	70.0	204.0	8.3/11.5	37.3	47.5	−10.2	*Gorshkov et al.* [1991]	7278
Mongolia	Taatsyn Gol 1–2	29.8	45.4	101.3	81.9	275.6	3.5/4.8	37.4	49.1	−11.7	this study	
India	Kargil	30.5	34.6	76.1	76.7	221.8	5.9/9.8	23.3	35.3	−12.0	*Klootwijk et al.* [1979]	615

Table 3. (continued)

	Basin/Terrane	Age (Mean)	Site Lat.	Site Long.	Paleopole Lat.	Paleopole Long.	dp/dm (A_{95})	Paleolatitude Observed	Experimental	ΔPlat	References	Result[a]
Average effusives small circle[e]		29.9 ± 0.5	41.9	93.2								
						16–22 Ma						
Europe APWP		20.0			84.0	154.8	2.7				*Besse and Courtillot* [2002]	
Sediments												
Tajikistan	Pulkhakim	19.5	38.1	67.4	69.0	277.5	8.5/15.0	19.4	38.1	−18.7	*Thomas et al.* [1994]	7491
Tajikistan	Pyrygata	19.5	37.7	68.2	60.0	299.0	7.5/13.5	16.2	37.8	−21.6	*Thomas et al.* [1994]	7490
Tajikistan	Kalinabad	19.5	38.0	69.0	42.0	328.5	6.0/10.0	17.8	38.2	−20.4	*Thomas et al.* [1994]	7488
Russia	West Siberia	19.5	60.0	83.0	70.0	230.0	4.7/6.1	42.1	61.4	−19.3	*Gorbunov* [1971]	3980
Tajikistan	Aksu	19.5	38.0	68.6	67.0	282.0	9.5/17.0	18.0	38.2	−20.2	*Thomas et al.* [1994]	7489
Kyrgyzstan	Northern Tien Shan	19.5	42.2	76.7	86.7	300.6	10.0/13.5	39.8	43.2	−3.4	*Thomas et al.* [1993]	7271
India	Jammu Foothills	20.0	34.3	73.9	56.5	335.0	5.0/8.5	23.5	35.0	−11.5	*Klootwijk et al.* [1986]	569
India	Jammu Foothills	20.0	34.3	73.9	50.0	324.0	6.5/12.5	14.5	35.0	−20.5	*Klootwijk et al.* [1986]	570
India	Jammu Foothills	20.0	33.1	74.3	71.0	203.5	3.5/6.0	20.1	33.9	−13.8	*Klootwijk et al.* [1986]	566
China	Yunnan Province	22.5	23.5	100.7	70.0	197.8	5.0/8.5	19.6	26.9	−7.3	*Haihong et al.* [1995]	7603
Tajikistan	Tukaynaron	22.5	38.8	69.6	47.5	323.0	7.0/12.5	18.2	39.0	−20.8	*Thomas et al.* [1994]	7487
India	Jammu Foothills	22.5	33.1	74.3	66.5	186.0	3.0/5.5	22.2	33.9	−11.7	*Klootwijk et al.* [1986]	567
Average sediments small circle[f]		20.4 ± 1.3	37.9	75.0								
						Effusives						
China	Shandong Province	16.0	36.4	118.8	86.6	236.1	4.9	34.8	41.2	−6.4	*Zhao* [1987]	7050
China	Shandong Province	16.0	36.3	118.6	85.2	238.4	5.6	33.8	41.1	−7.3	*Zhao et al.* [1994]	7227
South Korea		18.5	35.9	129.5	56.7	217.2	9.1	30.5	41.3	−10.8	*Kikawa et al.* [1994]	7220
Siberia	Ust Bokson	19.9	52.1	100.3	69.8	186.5	8.4/10.2	49.0	55.3	−6,3	this study	
China	Inner Mongolia	20.0	41.0	116.2	88.6	29.2	8.2	41.6	46.1	−4.5	*Zhao et al.* [1994]	7228
South Korea		20.5	36.0	129.5	64.5	222.1	10.4/15.5	31.0	41.4	−10.4	*Lee et al.* [1999]	8439
Mean effusives[g]		18.5 ± 2.0	40.0	119.7	86.6	268.7						
						7–15 Ma						
Europe APWP		10.0			85.4	162.5	2.0				*Besse and Courtillot* [2002]	
						Sediments						
West Nepal		7.0	28.0	82.0	72.2	267.5	1.1/2.1	10.3	28.7	−18.4	*Appel et al.* [1991]	6129
Pakistan	Potwar Plateau	7.5	32.8	73.2	57.4	326.6	3.1/5.4	19.1	32.7	−13.6	*Opdyke et al.* [1982]	1136
Pakistan	Potwar Plateau	7.5	32.8	72.5	75.8	279.9	2.9/5.0	20.0	32.7	−12.7	*Opdyke et al.* [1982]	1137
West Nepal		8.5	27.7	83.5	66.8	312.0	2.7/5.1	11.3	28.5	−17.2	*Gautam and Appel* [1994]	7095
West Nepal	Karnali River	10.5	28.7	81.3	69.5	290.5	1.5/2.9	10.5	29.3	−18.8	*Gautam and Fujiwara* [2000]	8537
West Nepal		10.5	28.9	80.7	65.6	297.6	2.0/3.8	8.7	29.5	−20.8	*Ojha et al.* [2000]	8557
Turkmenistan	Turan	11.0	39.0	58.0	69.0	204.0	6.1/10.5	20.9	37.7	−16.8	*Mammedov* [1971]	3978
Turkmenistan	Turan	12.5	38.0	58.5	76.0	238.0	7.4/12.2	24.0	36.8	−12.8	*Mammedov* [1971]	3975
Uzbekistan		12.5	40.5	70.7	73.0	263.0	4.0/7.0	23.8	40.2	−16.4	*Khramov and Slautsitais* [1982]	4080
Pakistan	Potwar Plateau	13.0	32.8	72.5	70.4	280.9	17.4/32.8	15.2	32.7	−17.5	*Johnson and Nigrini* [1985]	1142
Uzbekistan		14.0	40.0	70.0	73.0	244.0	2.0/4.0	23.1	39.6	−16.5	*Yeroshkin* [1982]	4076
Tajikistan	Tajik Depression	14.0	38.0	69.1	83.0	291.0	3.0/4.0	32.7	37.6	−4.9	*Khramov* [1970]	4087
Uzbekistan		14.0	40.0	70.0	72.0	259.0	1.0	22.2	39.6	−17.4	*Yeroshkin* [1982]	4075
Uzbekistan		14.0	41.0	72.0	73.0	298.0	3.0/5.0	15.8	39.0	−23.2	*Yeroshkin* [1982]	4078
China	Central Tarim	14.0	38.5	80.5	58.6	210.0	3.8/6.8	22.5	40.2	−17.7	*Dupont-Nivet et al.* [2002]	9009
Uzbekistan		14.0	40.5	70.5	71.0	230.0	1.0/2.0	28.3	40.8	−12.5	*Yeroshkin* [1982]	4077
China	Nan Shan Range	14.0	39.1	96.7	73.0	253.5	4.2/7	23.2	40.9	−17.7	*Dupont-Nivet et al.* [2003]	9168
Pakistan	Potwar Plateau	14.5	32.8	73.0	72.1	248.7	10.3/19.0	14.9	32.7	−17.8	*Wensink* [1972]	2853
China	Turfan Basin	14.5	43.0	89.6	66.8	255.1	5.1/5.1	20.4	44.2	−23.8	*Huang et al.* [2004]	9108
Uzbekistan	North Ferghana	14.5	41.2	71.9	83.0	288.0	1.0/1.4	35.4	41.0	−5.6	K. A. Abdullaev et al. (1993)[h]	6690
Uzbekistan	North Ferghana	14.5	41.0	72.8	74.0	292.0	7.5/11.6	28.0	40.9	−12.9	K. A. Abdullaev et al. (1993)	6688

Table 3. (continued)

	Basin/Terrane	Age (Mean)	Site Lat.	Site Long.	Paleopole Lat.	Paleopole Long.	dp/dm (A_{95})	Paleolatitude Observed	Experimental	ΔPlat	References	Result[a]
Uzbekistan	North Ferghana	14.5	41.1	72.2	84.0	261.0	1.0/1.4	35.2	40.9	−5.7	K. A. Abdullaev et al. (1993)	6689
Uzbekistan	North Ferghana	14.5	41.5	72.2	77.0	264.0	5.0/7.8	28.7	41.3	−12.6	K. A. Abdullaev et al. (1993)	6693
Average sediments small circle[i]		12.4 ± 2.6	37.1	74.6								
					Effusives							
Mongolia	Taatsyn Gol 3	12.7	45.5	101.0	71.6	178.0	14.6/18.2	46.6	47.5	−0.9	this study	
Mongolia	Zavhan	14.0	46.5	96.5	77.0	162.0	19.2/23.5	50.4	48.2	2.2	*Gorshkov et al.* [1991]	7277
China	Hebei Province	15.0	41.0	114.7	83.4	192.8	6.2/6.2	42.0	44.0	−2.0	*Zheng et al.* [1991]	5719
Mean effusives[j]		13.9 ± 0.9	44.6	104.4	77.6	175.1						

[a]Result number as given in the "RESUTNO" field of the Global Paleomagnetic Database.
[b]For $\theta = 78.1° \pm 2.7°$, n = 14, and average ΔPlat.
[c]For $\theta = 63.2° \pm 2.8°$, n = 4, and average ΔPlat.
[d]For $\theta = 70.8 \pm 2.6$, n = 17, and average ΔPlat.
[e]For $\theta = 56.9 \pm 1.7$, n = 3, and average ΔPlat.
[f]For $\theta = 68.9 \pm 4.2$ n = 12, and average ΔPlat.
[g]For $A_{95} = 3.1$ and average ΔPlat.
[h]Paleomagnetic directions and paleomagnetic pole positions: Data for the former USSR, VNIGRI Institute, St. Petersburg, unpublished.
[i]For $\theta = 68.1 \pm 2.0$ n = 23, and average ΔPlat.

the means listed in Table 2 have been computed using *Fisher* [1953] statistics. Because of a poor separation of magnetic components during demagnetization processes, 27% of the flow-mean directions were computed using the mixed average of directional data and great circles of *McFadden and McElhinny* [1988]. Finally, two sites (08 at TG3 and 92 at Khaton-Sudal) provided only mean remagnetization great circles.

[21] At Khaton-Sudal (Figure 7a), as the great circles of site 92 are parallel to one another, we have computed an average great circle using the tensor bivariate statistics of *Le Goff* [1990], the normal of which is reported in Table 2. Thus we have computed the mean formation of Khaton-Sudal including this average great circle (Figure 7a), using the statistics of *McFadden and McElhinny* [1988]. All the other HTC site-mean directions exhibit reverse polarities. This is consistent with the age of 39.4 ± 0.6 Ma we obtained by K-Ar dating, suggesting that this volcanic edifice was emplaced during the geomagnetic field reverse period C18n.1r [*Cande and Kent*, 1995; *Gradstein et al.*, 2004]. The formation mean direction (white star with gray area of confidence, Figure 7a) is distinct from the present-day dipole (gray star) and IGRF 2000 (gray diamond) magnetic fields (in reverse polarity). We thus conclude we have recovered the primary magnetization of this formation, reflecting the magnetic field vector at this location at 39.4 ± 0.6 Ma. The corresponding paleopole (Figure 8 and Table 3), computed from this average HTC, lies at $\lambda = 72.0°$N, $\phi = 202.6°$E (dp/dm = 6.3°/8.5°), which provides a middle Eocene paleolatitude of 38.6° ± 6.3°N for the Khaton-Sudal area.

[22] The HTC flow mean directions of Taatsyn Gol 1 (TG1, 31.5 Ma) are all of reverse polarity (Figure 7b and Table 2), consistent with the reverse magnetic field during chron C12 within the early Oligocene (Rupelian [*Cande and Kent*, 1995; *Gradstein et al.*, 2004]). One site (74, white triangle in Figure 7b) has been excluded from the final mean computation because it is clearly an outlier. Examination of Figure 7b shows that TG1 HTC directions are well clustered. This high degree of clustering and the single polarity suggest that the period of flow emplacements at TG1 was fairly short. Consequently, the magnetic field paleosecular variation may not be fully averaged out by our sampling. The same observation holds for Taatsyn Gol 2 (TG2, 28.0 Ma), which also shows a high degree of clustering of flow site-mean directions, but in normal polarity (Figure 7b and Table 2). It should be noticed that even though both TG2 and TG1 groups possibly represent short temporal sampling intervals of the magnetic field and show normal and reverse polarities, they are not exactly antiparallel and fail the reversal test of *McFadden and Lowes* [1981]. Nonetheless, in order to obtain a paleopole at ~30 Ma close to the dipole field, we have chosen to combine flows from TG2 (28.0 Ma) and TG1 (31.5 Ma) localities (mean age 29.8 Ma). The obtained mean direction (black star with gray area of confidence, Figure 7b) does not contain either the present-day dipole or IGRF magnetic field directions (gray star and diamond, Figure 7b) and is our best estimate of

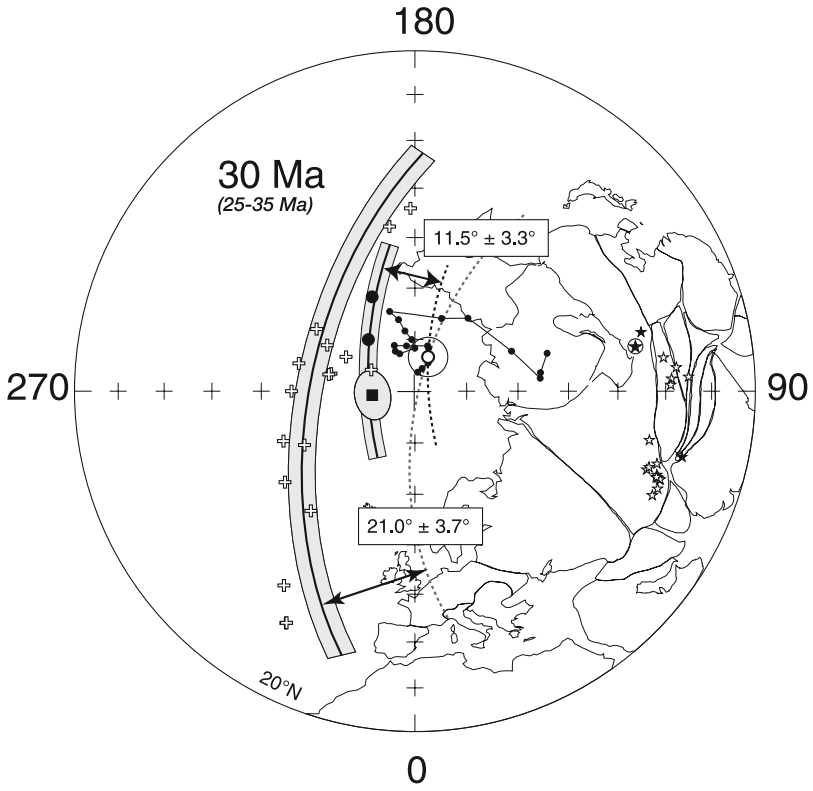

Figure 9. Equal-area projection of the Earth's northern hemisphere limited to the 20°N latitude showing the 29.8 Ma Taatsyn Gol 1 and 2 paleopole (black square with shaded dp/dm ellipse of confidence) and selected paleopoles within the 25–35 Ma time interval. White dot with A_{95} circle of confidence indicates 30 Ma Europe APWP pole; circled black star indicates Taatsyn Gol locality. Otherwise, small circles, white and black symbols are as in Figure 8.

the magnetic field direction at 30 Ma. The paleopole computed from this HTC average (Figure 9 and Table 3) is located at λ = 81.9°N, ϕ = 275.6°E (dp/dm = 3.5°/4.8°), providing a paleolatitude of 37.4° ± 3.5°N at ~30 Ma for the Taatsyn Gol area.

[23] We encounter the same problem with Ust Bokson data (Figure 7c and Table 2) which cluster into a group of normal polarity in six flows from the western bank of Oka River (19.9 Ma) and a group of reverse polarity from three flows of the eastern bank (19.8 Ma). This is consistent with the high reversal frequency of chron C6 in the early Miocene [*Cande and Kent*, 1995; *Gradstein et al.*, 2004]. Here again, the high cluster in each population and the failure of the reversal test [*McFadden and Lowes*, 1981] suggests that paleosecular variation might not have been fully averaged out. As for TG1-2 populations, our best estimate of the dipole field is to compute an average from the nine flows. The formation mean direction is shown in Figure 7c (black star with gray area of confidence). It is distinct from both present-day dipole and IGRF magnetic fields directions (gray star and diamond, Figure 7c) and is assumed to be the magnetic field direction at 19.8 Ma. The corresponding paleopole (Figure 10 and Table 3) lies at λ = 69.8°N, ϕ = 186.5°E (dp/dm = 8.4°/10.2°), corresponding to a ~20 Ma paleolatitude for the Ust Bokson area of 49.0° ± 8.4°N.

[24] HTC directions from Taatsyn Gol 3 (TG3, 12.7 Ma) are all of reverse polarity (Figure 7d and Table 2). Accounting for the high frequency of magnetic field reversals during chron C5 of middle Miocene, this could indicate a rather short time interval of flow emplacement (<~200 kyr). However, the population appears more scattered than in previous cases and the VGP scatter computed from the seven flows is in line with the scatter due to paleosecular variation, as modeled by *McFadden et al.* [1991] for this period. Thus the formation mean direction of TG3 (white star with gray area of confidence, Figure 7d), which is again distinct from both the present-day dipole and IGRF fields at this location, is thought to provide the magnetic field direction for this locality at 12.7 Ma. This leads us to compute a paleopole (Figure 11 and Table 3) at λ = 71.6°N, ϕ = 178.0°E (dp/dm = 14.6°/16.8°), with a ~13 Ma paleolatitude of 46.6° ± 14.6°N for the Taatsyn Gol area.

5. Analysis of Paleopoles

[25] The computed paleopoles from paleomagnetic results are given in Table 3 and illustrated in Figures 8 through 11. They are compared to coeval poles from central Asia, in a large sense (i.e., delimited to the west by Afghanistan, to the east by China blocks, to the south by India, and to the north by Siberia). The selected paleopoles were taken from the Global Paleomagnetic Database of *McElhinny and Lock* [1996] (version 4.6, February 2005), using the following criteria: paleopoles should be based on (1) more than two

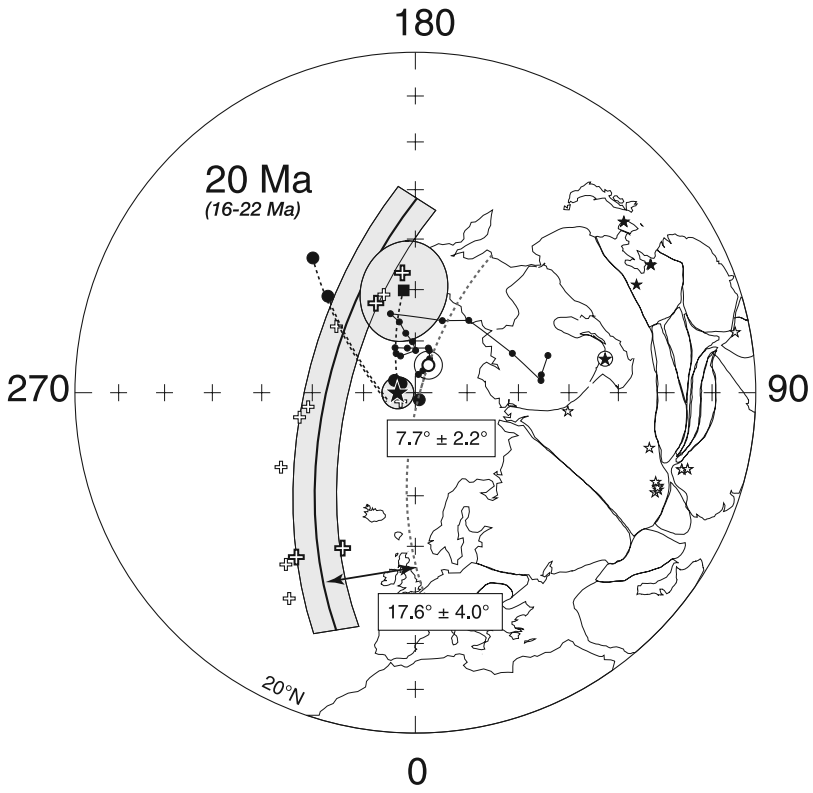

Figure 10. Equal-area projection of the Earth's northern hemisphere limited to the 20°N latitude showing the 19.9 Ma Ust Bokson paleopole (black square with shaded dp/dm ellipse of confidence) and selected paleopoles within the 16–22 Ma time interval. Large black star with shaded A_{95} circle of confidence indicates average 20 Ma (18.5 ± 2.0 Ma; Table 3) pole from effusive formations, computed after a mixed average between small circles passing through Ust Bokson and South Korea poles (dotted lines) and paleopoles from NCB (see text); this pole shows a 7.7° ± 2.2° far-sided offset from the 20 Ma reference pole (white dot with A_{95} circle of confidence) with respect to average site location. Circled black star indicates Ust Bokson locality. Otherwise, small circles, white and black symbols are as in Figure 8.

sites and/or 20 specimens, (2) thermal demagnetization of sediments, (3) an A_{95} area of confidence, or a *dp* angle, lower than 16°, and (4) formations not suspected of later remagnetization. We have split this collection into four age groups centered on 40 Ma (from 35 to 45 Ma), 30 Ma (25–35 Ma), 20 Ma (16–22 Ma) and 13 Ma (7–15 Ma). In Figures 8 to 11 and Table 3, different symbols are used to represent data obtained on sedimentary formations (white symbols in Figures 8 to 11), as opposed to effusive formations (black symbols). Finally, data originating from the India plate are also highlighted (bold symbols in Figures 8 to 11). In the following, we discuss the Inclination Anomaly problem in terms of paleopole positions relative to the reference APWP poles for each epoch [*Besse and Courtillot*, 2002], rather than taking analytical approach of observed versus expected paleomagnetic inclination at each locality.

5.1. Paleopoles From Sedimentary Formations

[26] Overall, our first observation is that there are many more data coming from sedimentary formations, with a total of 66 paleopoles listed in Table 3, than from effusive formations (16 paleopoles, Table 3). Furthermore, paleopoles from sedimentary formations (white plus symbols, Figures 8 to 11) are located systematically on the far side of the reference poles from the European APWP at 40, 30, 20, and 10 Ma, with respect to site localities (white stars). Second, due to the ongoing indentation of Eurasia by India during the Tertiary, many of the localities have undergone local rotations around vertical axes, leading to an overall small circle distribution of paleopoles for a given age. We have computed the average small circles passing through paleopoles from sedimentary formations (Table 3 and Figures 8 to 11) and centered on the average site locations. These small circles show that the offset between observed and predicted paleopoles, computed following *Coe et al.* [1985], amount to 20.9° ± 3.4° at ~40 Ma (Figure 8), 21.0° ± 3.7° at ~30 Ma (Figure 9), 17.6° ± 4.0° at ~20 Ma (Figure 10), and 15.2° ± 1.6° at ~13 Ma (Figure 11).

[27] This observation, in itself, describes the Inclination Anomaly of Asia, since the far-sided offset of poles results from inclinations, which are shallower than those expected from the reference APWP at each locality. In the hypotheses of (1) a rigid Eurasian continent, allowing the use of the European APWP [*Besse and Courtillot*, 2002] as a reference for Siberia craton, (2) a dipolar magnetic field, and (3) a conformity between paleomagnetic and geomagnetic vectors at the time of sediments deposition and/or magnetization acquisition by sediments, the far-sided offsets would imply latitudinal displacement of 2300 ± 400 km of northward convergence of the Asian blocks (as a whole) with respect to Siberia since 40 and 30 Ma (at velocities of

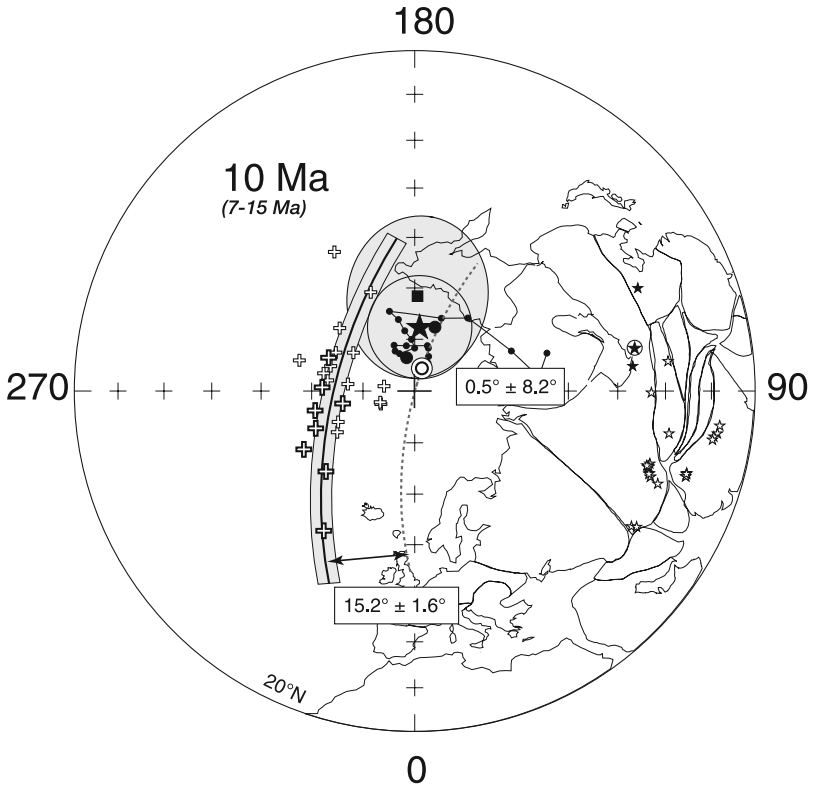

Figure 11. Equal-area projection of the Earth's northern hemisphere limited to the 20°N latitude showing the 12.7 Ma Taatsyn Gol 3 paleopole (black square with shaded dp/dm ellipse of confidence) and selected paleopoles within the 7–15 Ma time interval. Large black star with shaded A_{95} circle of confidence indicates average 13 Ma (13.9 ± 0.9 Ma; Table 3) pole from effusive formations showing insignificant far-sided offset of 0.5° ± 8.2° with respect to the 10 Ma pole (white dot with A_{95} circle of confidence) of Europe APWP. Circled black star indicates Taatsyn Gol locality. Otherwise, small circles, white and black symbols are as in Figure 8.

57.5 and 76.7 mm/yr, respectively), 1950 ± 440 km since 20 Ma (average velocity 97.5 mm/yr), and even worse, 1690 ± 180 km since 13 Ma (at an average velocity of 130.0 mm/yr). These values are indeed unrealistic given the total amount of intracontinental shortening required and the plate velocities implied. As discussed, in particular by *Cogné et al.* [1999], several other causes, apart from the probable intracontinental shortening due to India's penetration into Eurasia, must be invoked, amongst which an inclination shallowing due to sedimentary processes which could lead to this anomaly [e.g., *Gilder et al.*, 2001; *Tan et al.*, 2003]. We now turn our discussion to the analysis of the distribution of paleopoles obtained on effusive formations, including our four new poles, for which inclination shallowing due to sedimentary processes is avoided.

5.2. Paleopoles From Effusive Formations

[28] The 39.4 Ma paleopole of Khaton-Sudal (Figure 8) lies at an angular distance of 12.6° ± 7.1° from the 40 Ma reference pole from Europe APWP [*Besse and Courtillot*, 2002]. This angle can be decomposed into (1) a component of clockwise (CW) rotation of the locality around a vertical axis of Rot = 11.4° ± 9.5°, and (2) a far-sided offset of $\Delta\lambda$ = 9.6° ± 5.7° which results from a shallowing of ΔInc = 8.0° ± 4.7° of observed paleomagnetic inclination with respect to the expected one. The far-sided position of our Khaton-Sudal (KS) pole appears consistent with three other late Eocene poles from Tajikistan, Kyrgyzstan and Afghanistan (Table 3). Here again, because of relative vertical axis rotations between localities, the four poles align on a small circle (Figure 8). The small circle passing through these poles and centered on the average sites location, shows a bulk far-sided offset of 13.9° ± 3.5° with respect to the 40 Ma reference pole (Figure 8). Inclination shallowing due to sedimentary processes cannot be invoked for these effusive rocks. Furthermore, it is difficult to interpret the accommodation of this offset of poles by a ~1100–1500 km of intracontinental shortening between Amuria block and Siberia after 40 Ma, because (1) our KS locality is located in the north of the Asian mosaic, very close to south Siberia, and (2) there are no high mountain ranges in the Trans Baikal area. Therefore we conclude that the European APWP might not be valid for the Siberia craton. Considering a dipolar magnetic field, hypothesis discussed below, this would suggest that Siberia was located 1100–1500 km more to the south than its predicted position in the Eocene, as proposed by *Cogné et al.* [1999]. Finally, we note that if we take the paleopoles of effusive formations as a reference, the bulk 20.9° ± 3.4° far-sided offset of paleopoles from sedimentary formations reduces to a much more reasonable

value of $\Delta\lambda = 7.0° \pm 3.9°$ (radial difference between the two small circles in Figure 8). This ~800 km offset of sediment poles with respect to effusive poles probably results from the superimposition of two effects: inclination shallowing due to sedimentary processes and intracontinental shortening between Siberia and India since 40 Ma.

[29] The same analysis holds for 30 Ma poles (Figure 9). The 29.8 Ma pole, obtained from basalts at the Taatsyn Gol 1 and 2 (TG1-2) localities, lies at an angular distance of $13.1° \pm 5.2°$ from the 30 Ma European APWP pole, indicative of a slight counterclockwise (CCW) rotation of Rot = $-8.2° \pm 7.3°$ and a significant far-sided offset of $\Delta\lambda = 11.7° \pm 4.1°$ (corresponding to ΔInc = $9.7° \pm 3.3°$). There are only two other published results from effusive rocks for this period. We compare (Table 3 and Figure 9) our pole with a pole obtained from basalts at Khan Uul in Mongolia [*Gorshkov et al.*, 1991] and a pole obtained from intrusive rocks at Ladakh [*Klootwijk et al.*, 1979]. Although the Mongolian pole is based on only 22 specimens and the Ladakh pole is obtained on intrusives for which the paleohorizontal may be poorly constrained, especially in this tectonized area, they both fit a small circle distribution with our TG1-2 pole. The far-sided offset amounts to $11.5° \pm 3.3°$ with respect to the 30 Ma reference pole. As above, we therefore conclude that Siberia might have been located ~1300 km farther south than its expected paleoposition based on the European APWP at 30 Ma. Here again, we note that if the effusive poles are taken as a reference, the inclination anomaly in sediments, reflected by a $21.0° \pm 3.7°$ far-sided offset of poles with respect to Europe APWP, is divided by 2, leading to a remaining offset of $\Delta\lambda = 9.5° \pm 3.9°$.

[30] Paleomagnetic analysis at 20 Ma (Figure 10) is less straightforward. Our Ust Bokson (UB) pole at 19.9 Ma still does not conform to the reference pole at 20 Ma from the European APWP. The angular distance between the paleopoles and reference poles is $15.4° \pm 8.8°$, suggesting a CW rotation of UB pole about a local vertical axis of Rot = $23.1° \pm 13.7°$ and a far-sided offset of $\Delta\lambda = 6.3° \pm 7.1°$ (corresponding to ΔInc = $4.4° \pm 5.3°$). The large CW rotation of the Ust Bokson locality is somewhat difficult to assess. It could be linked to its proximity to the Mongol-Okhotsk suture zone believed to be a large transpressionnal sinistral megashear during the Tertiary, as discussed by *Halim et al.* [1998a] and *Cogné et al.* [2005]. Albeit far-sided, the offset of UB pole could be regarded as insignificant considering the confidence limits. However, we make the following analysis. Five other poles from effusive formations at ~20 Ma can be found in the literature (Table 3): three of them come from the North China Block (NCB [*Zhao and Coe*, 1987; *Zhao et al.*, 1994]), and two are from South Korea (SK [*Kikawa et al.*, 1994; *Lee et al.*, 1999]). It appears that the NCB poles have not undergone significant rotations with respect to European APWP pole since 20 Ma (Figure 10), which is in contradictions with our UB pole, as well as SK poles, both having suffered significant CW rotations. For this reason, and because the NCB has not undergone any significant northward motion with respect to Siberia since the Mongol-Okhotsk Ocean closure, end of the Jurassic [*Enkin et al.*, 1992; *Kravchinsky et al.*, 2002; *Cogné et al.*, 2005], we attempt to compute an average ~20 Ma pole for Asia, using the mixed statistics between fixed poles of NCB and small circles passing through SK and UB (black star with light gray A_{95} circle of confidence, Figure 10). This pole lies at (Table 3) $\lambda = 86.6°$, $\phi = 268.7°$ (n = 6, k = 547.1, A95 = 3.1°, mean age = 18.5 ± 2.0 Ma). Attributed to the average site location of these six localities ($\lambda = 40.0°$, $\phi = 119.7°$), the pole shows a $8.0° \pm 2.7°$ discrepancy with respect to the 20 Ma reference pole of Europe APWP, resulting from an insignificant average local CCW rotation of Rot = $-2.7° \pm 3.8°$ and a far-sided offset of $\Delta\lambda = 7.7° \pm 2.2°$ (average shallow inclination anomaly, ΔInc = $6.8° \pm 1.7°$). Altogether, we observe that the ~850 km far-sided offset of the ~20 Ma paleopoles from effusive formations of Asia has diminished with respect to the offset at ~40 Ma (1100 to 1500 km) and at ~30 Ma (~1300 km). More importantly, we underline that effusive poles at 20 Ma are still inconsistent with the reference pole of Europe APWP. They would imply a paleoposition of Siberia ~850 km farther south than expected. Accordingly, the offset of poles from sedimentary formations has passed from 20.9° and 21.0° at 40 and 30 Ma, respectively (Figures 8 and 9), to 17.6° at 20 Ma (Figure 10). Thus the difference in offset between sedimentary and effusive formations poles remains quite constant at $\Delta\lambda = 9.9° \pm 3.6°$ at 20 Ma, reducing the anomaly.

[31] Our 12.7 Ma paleopole from the Taatsyn Gol 3 (TG3) location has quite a large dp/dm ellipse of confidence (Figure 11 and Table 3) which contains the reference pole of Europe APWP at 10 Ma. In effect, the angular distance between these two poles ($14.0° \pm 13.8°$) as well as rotation (Rot = $20.6° \pm 20.2°$) and offset ($\Delta\lambda = 0.9° \pm 11.1°$, corresponding to ΔInc = $0.7° \pm 8.6°$) are consistent with the reference pole at 10 Ma for Europe, with perhaps a CW rotation of Taatsyn Gol area with respect to Siberia. This means that since that age, the anomaly is not apparent and the Europe APWP conveniently describes the paleoposition of the Siberia craton. Two other poles from effusive formations from Mongolia and NCB (Table 3) are in line with this observation. The mean ~13 Ma pole (13.9 ± 0.9 Ma, Table 3; black star with light gray A_{95} area in Figure 11) lies at $\lambda = 77.6°$, $\phi = 175.1°$ (N = 3, k = 153.0, $A_{95} = 10.0°$). It also shows insignificant differences with the 10 Ma reference pole with an angular distance of $8.0° \pm 10.2°$, Rot = $11.7° \pm 15.1°$ (CW) and $\Delta\lambda = -0.5° \pm 8.2°$ (far-sided), corresponding to an inclination shallowing of ΔInc = $0.4° \pm 6.3°$. We can therefore assume that at that time, the Inclination Anomaly of central Asia has disappeared. However, poles from sedimentary formations still show a significant offset, which amounts to $14.9° \pm 6.7°$, and should probably be attributed, for in large part, to sedimentary processes.

5.3. Paleolatitudes

[32] All the above analysis of paleopole distributions can be expressed in another way. For each pole listed in Table 3, we have computed the observed paleolatitude ($Plat_{obs}$) deduced from paleomagnetic data, and the expected paleolatitude ($Plat_{exp}$) deduced from Europe APWP [*Besse and Courtillot*, 2002] for each time period and for the present-day latitude of localities. The differences in paleolatitudes, computed as $\Delta Plat = Plat_{obs} - Plat_{exp}$ are given in Table 3 and illustrated in Figure 12. A negative ΔPlat indicates an observed paleolatitude, which is farther south than expected. We make the following observations. (1) All the

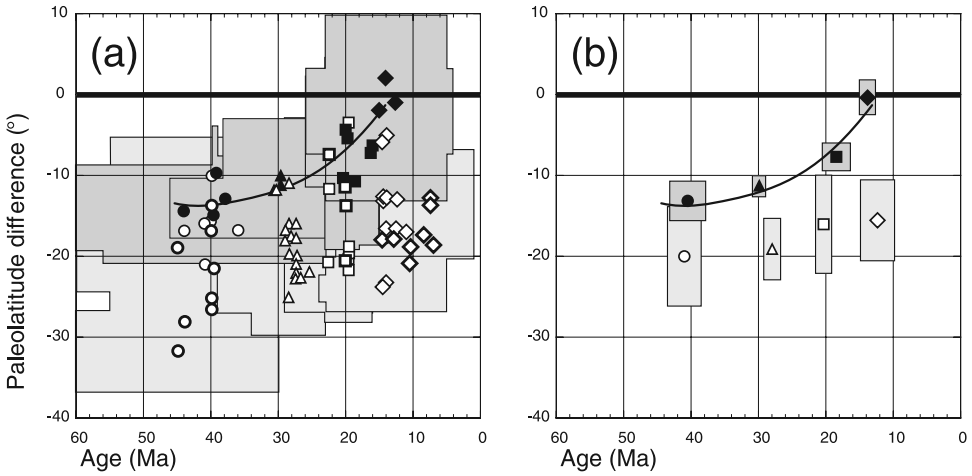

Figure 12. Paleolatitude differences computed as ΔPlat = $Plat_{obs}$ − $Plat_{exp}$, with $Plat_{obs}$ ($Plat_{exp}$), observed (expected) paleolatitudes of paleomagnetic sampling sites, as a function of time from 60 Ma to the Present for (a) all the data of Table 3 and (b) their means with shaded areas of uncertainty. White (black) symbols indicate data from sedimentary (effusive) formations. Bold white symbols indicate data from the India plate; dots, 35–45 Ma time interval; triangles indicate 25–35 Ma; squares indicate 16–22 Ma; diamonds indicate 7–15 Ma. The black thin curve underlines the diminishing paleolatitude anomaly of effusive formation data with time, from 40 to 13 Ma.

points, except one, show negative ΔPlat within the uncertainty field (Figure 12a). (2) ΔPlat values for effusive formations are systematically negative (except for the most recent ~13 Ma period). Although sampling of effusive formations may lead to an insufficient averaging of paleosecular variation, the systematic offset of points shown in Figure 12 provides a strong argument against that possibility at this level of analysis. (3) Although there is some overlap between the two populations, ΔPlat values of effusive formations are systematically lower than those deduced from sedimentary formations (Figure 12a). This is confirmed by computing average values for each time period (Figure 12b). (4) The ΔPlat values of effusive formations diminish with time (Table 3 and Figure 12b). (5) The ΔPlat difference between sedimentary and effusive formations is quite constant during the 40–20 Ma period and amounts to 6.8° ± 6.5° at ~40 Ma, 7.7° ± 4.0° at ~30 Ma, and 8.2° ± 6.3° at ~20 Ma. Only the data at ~13 Ma show a higher difference of 15.2° ± 5.5°.

6. Discussion

[33] From the middle Eocene to the early Miocene, paleopoles obtained from effusive formations, including our new poles at 39.4, 29.8, and 19.9 Ma, are systematically far sided from the European APWP [*Besse and Courtillot*, 2002] with respect to site locations. This implies that paleomagnetic inclinations within these effusive rocks are shallower than expected from the reference APWP. Since (1) no inclination shallowing mechanism due to sedimentary processes can be evoked in these effusive formations and (2) formations are well dated and no age error can be suspected, the causes for such low inclinations are either an anomaly of the magnetic field or an undetected tectonic setting which would allow Siberia (and all the other central Asia blocks) to be located farther south than expected from the reference APWP of Europe for that time period. For the Tertiary of Eurasia, the most commonly invoked anomaly is a long-lasting nondipole field due either to a rapid global shift of the dipole [*Westphal*, 1993], to local field anomalies [*Chauvin et al.*, 1996], or to the persistence, during the Cenozoic, of quadrupole and octupole terms in the magnetic field [*Si and Van der Voo*, 2001; *Van der Voo and Torsvik*, 2001; *Torsvik and Van der Voo*, 2002]. However, recent analyses of the global paleomagnetic database [*Besse and Courtillot*, 2002; *Courtillot and Besse*, 2004] lead to estimates of only 3% ± 2% of quadrupole contribution to the global magnetic field during the last 200 m.y., leading to an average 1.4° ± 1.2° far-sided offset of paleomagnetic poles with respect to geographic north.

[34] Conversely, *Cogné et al.* [1999] proposed an alternative hypothesis based on tectonics, where in the hypothesis of a dipolar magnetic field, "stable" Siberia could have been located farther south than its expected paleolatitude, in the Tertiary. On the basis of our new poles from the northern parts of the Asian system, thus avoiding problems linked to Cenozoic tectonics related to India indentation, and also on coeval poles from Asia, we here follow this line and propose the following. At ~40 Ma, Siberia (and all the other Asian blocks) is located 1450 ± 250 km south of its expected paleolatitude from the European APWP of *Besse and Courtillot* [2002]. At ~30 Ma, this difference is still 1250 ± 100 km, then it decreases to 850 ± 200 km at ~20 Ma and vanishes (with 20 ± 200 km) at ~13 Ma.

[35] This scenario has several consequences. First, because there is an overall consistency of Cretaceous poles from Asia with the European APWP, taking into account Asia tectonics [*Molnar and Tapponnier*, 1975; *Tapponnier and Molnar*, 1979; *Tapponnier et al.*, 1986; *Zhao and Coe*, 1987; *Zhao et al.*, 1990; *Enkin et al.*, 1992; *Avouac and Tapponnier*, 1993; *Chen et al.*, 1993a; *Ma et al.*, 1993; *Yang and Besse*, 1993; *Chen et al.*, 1993b; *Gilder et al.*, 1996; *Gilder and Courtillot*,

1997; *Halim et al.*, 1998a, 1998b; *Yang et al.*, 2001; *Yang and Besse*, 2001; *Chen et al.*, 2002; *Kravchinsky et al.*, 2002; *Gilder et al.*, 2003], the Cenozoic discrepancy, described above, implies a nonrigidity of the Eurasian plate since the Cretaceous. This nonrigidity of Eurasia was supposed to be absorbed into discrete zones such as the Tornquist-Tesseyre line, and the Ural mountain ranges. Although it is not the subject of the present study, we note that *Puchkov* [1997] reported that Uralian-Cimmerian mountain belt was eroded and partially inundated by seas during the Late Jurassic–Early Cretaceous and has been reactivated since the Oligocene. This is consistent with the idea of a tectonic activity within central Eurasia, decoupling western Europe from eastern Eurasia, during the Cenozoic.

[36] We now turn to the inclination anomaly in sediments from Asia. Because our analysis of effusive poles suggest that Siberia was located 850–1450 km farther south than its expected paleolatitude in the 20–40 Ma period, the paleolatitude anomaly from sedimentary formations (Table 3) is strongly reduced. In effect, taking effusive poles as a reference, this anomaly would be reduced to 750 ± 720 km, 850 ± 450 km, and 900 ± 700 km in paleolatitudes at ~40, 30, and 20 Ma, respectively. This (much reasonable) anomaly could result from the superimposition of (1) a paleomagnetic inclination shallowing mechanism due to sedimentation processes such as compaction [e.g., *Tan et al.*, 2003] or imbrication [e.g., *Gilder et al.*, 2001] to (2) a most probable northward movement of Asian blocks due to the ongoing penetration of India into Eurasia since 50 Ma. From the present analysis, we are not able to go further in deciphering between these two causes. Finally, the ~13 Ma poles from sedimentary formations are not in line with this analysis. If one considers that our effusive TG3 pole, together with coeval poles, are consistent with the reference APWP, then the bulk 1700 ± 600 km paleolatitude anomaly of 7–15 Ma sedimentary localities appears truly anomalous and is hardly explained by a combination of inclination shallowing and northward movement. Further investigations are definitely needed to solve this problem.

[37] Finally, although our new poles from Mongolia and south Siberia, together with the analysis of previously published paleomagnetic poles from Asia provide herein, allow to elucidate some aspects of the Tertiary inclination anomaly problem in central Asia since 40 Ma, there is still a need to combine this analysis of Tertiary data with Cretaceous ones. Furthermore, a temporal gap remains in this analysis between ~100 and 40 Ma, which should be investigated in order to have a complete characterization of the Inclination Anomaly in Asia.

[38] **Acknowledgments.** We wish to thank O. Tamurtogoo, G. Badarch, and J. Badamgarav from Geological Institute of Mongolian Academy of Sciences for efficient organization and guiding in the field during 1999 expedition to Gobi desert and Uyanga, Khatna, and Moogii for their efficient help during the 2004 field expedition. X. Quidelleur, A. Hildenbrand, and J. C. Lefèvre kindly assisted F.H. for K-Ar dating of Khaton Sudal samples. F. Lagroix helped us edit this paper, and the present version largely benefited from numerous and constructive reviews by R. Enkin and Y. Otofuji. This is contribution 2168 of IPGP.

References

Appel, E., W. Rosler, and G. Corvinus (1991), Magnetostratigraphy of the Miocene-Pleistocene Surai Khola Siwaliks in west Nepal, *Geophys. J. Int.*, *105*, 191–198.

Avouac, J. P., and P. Tapponnier (1993), Kinematic model of active deformation in central Asia, *Geophys. Res. Lett.*, *20*, 895–898.

Barry, T. L., and R. W. Kent (1998), Cenozoic magmatism in Mongolia and the origin of central and east Asian basalts, in *Mantle Dynamics and Plate Interactions in East Asia*, *Geodyn. Ser.*, vol. 27, edited by M. F. J. Flowers et al., pp. 347–364, AGU, Washington, D. C.

Barry, T. L., A. D. Saunders, P. D. Kempton, B. F. Windley, M. S. Pringle, D. Dorjnamjaa, and S. Saandar (2003), Petrogenesis of Cenozoic basalts from Mongolia: Evidence for the role of asthenospheric versus metasomatized lithospheric mantle sources, *J. Petrol.*, *44*, 55–91.

Bazhenov, M. L. and V. S. Burtman (1990), *Structural arcs of the Alpine Belt: Carpathians-Caucasus-Parmir* (in Russian), 168 pp., Nauka Moscow.

Bazhenov, M. L., V. S. Burtman, and G. Z. Gurariy (1978), Studies of the curvature of the Parmir arc in the Paleogene using the paleomagnetic method, *Dokl. Acad. Sci. USSR*, *242*, 1137–1139.

Besse, J., and V. Courtillot (1991), Revised and synthetic apparent polar wander paths of the African, Eurasian, North American, and Indian plates and true polar wander since 200 Ma, *J. Geophys. Res.*, *96*, 4029–4050.

Besse, J., and V. Courtillot (2002), Apparent and true polar wander and the geometry of the geomagnetic field over the last 200 Myr, *J. Geophys. Res.*, *107*(B11), 2300, doi:10.1029/2000JB000050.

Cande, S. C., and D. V. Kent (1995), Revised calibration of the geomagnetic polarity timescale for the Late Cretaceous and Cenozoic, *J. Geophys. Res.*, *100*, 6093–6095.

Cassignol, C. and P.-Y. Gillot (1982), Range and effectiveness of unspiked potassium-argon dating, in *Numerical Dating in Stratigraphy*, edited by G. S. Odin, pp. 159–172, John Wiley, Hoboken, N. J.

Chauvin, A., H. Perroud, and M. L. Bazhenov (1996), Anomalous low paleomagnetic inclinations from Oligocene-lower Miocene red beds of south-west Tien Shan, central Asia, *Geophys. J. Int.*, *126*, 303–313.

Chen, Y., J. P. Cogné, and V. Courtillot (1992), New Cretaceous paleomagnetic poles from the Tarim Basin, northwestern China, *Earth Planet. Sci. Lett.*, *114*, 17–38.

Chen, Y., J. P. Cogné, V. Courtillot, P. Tapponnier, and X. Y. Zhu (1993a), Cretaceous paleomagnetic results from western Tibet and tectonic implications, *J. Geophys. Res.*, *98*, 17,981–17,999.

Chen, Y., V. Courtillot, J.-P. Cogné, J. Besse, Z. Yang, and R. Enkin (1993b), The configuration of Asia prior to the collision of India: Cretaceous paleomagnetic constraints, *J. Geophys. Res.*, *98*, 21,927–21,941.

Chen, Y., H. Wu, V. Courtillot, and S. Gilder (2002), Large N-S convergence at the northern edge of the Tibetan Plateau? New Early Cretaceous paleomagnetic data from Hexi Corridor, NW China, *Earth Planet. Sci. Lett.*, *201*, 293–307.

Coe, R. S., B. R. Globerman, P. W. Plumley, and G. A. Thrupp (1985), Paleomagnetic results from Alaska and their tectonic implications, in *Tectonostratigraphic Terranes of the Circum-Pacific Region*, edited by D. G. Howell, pp. 85–108, Circum-Pac. Counc. for Energy and Miner. Resour., Houston, Tex.

Cogné, J. P. (2003), PaleoMac: A Macintosh™ application for treating paleomagnetic data and making plate reconstructions, *Geochem. Geophys. Geosyst.*, *4*(1), 1007, doi:10.1029/2001GC000227.

Cogné, J. P., N. Halim, Y. Chen, and V. Courtillot (1999), Resolving the problem of shallow magnetizations of Tertiary age in Asia: Insights from paleomagnetic data from the Qiangtang, Kunlun, and Qaidam blocks (Tibet, China), and a new hypothesis, *J. Geophys. Res.*, *104*, 17,715–17,734.

Cogné, J. P., V. Kravchinsky, N. Halim, and F. Hankard (2005), Late Jurassic-Early Cretaceous closure of the Mongol-Okhotsk Ocean demonstrated by new Mesozoic paleomagnetic results from the Trans-Baïakal area (SE Siberia), *Geophys. J. Int.*, *163*, 813–832.

Courtillot, V., and J. Besse (2004), A long-term octupolar component in the geomagnetic field? (0–200 million years B.P.), in *Timescales of the Paleomagnetic Field*, *Geophys. Monogr. Ser.*, vol. 145, edited by J. E. T. Channell et al., pp. 59–74, AGU, Washington, D. C.

Cunningham, W. D. (2001), Cenozoic normal faulting and regional doming in the southern Hangay region, Central Mongolia: Implications for the origin of the Baikal rift province, *Tectonophysics*, *331*, 389–411.

Davydov, V. F., R. A. Komissarova, and A. N. Khramov (1986), Paleomagnetic directions and pole positions: Data for the USSR, in *World Data Center-B Catalogue*, Sov. Geophys. Comm., Moscow.

Dunlop, D. J. (2002), Theory and application of the Day plot (M_{rs}/M_s versus H_{cr}/H_c) 1. Theoretical curves and tests using titanomagnetite data, *J. Geophys. Res.*, *107*(B3), 2056, doi:10.1029/2001JB000486.

Dupont-Nivet, G., R. F. Butler, A. Yin, and X. Chen (2002), Paleomagnetism indicates no Neogene rotation of the Qaidam Basin in northern Tibet during Indo-Asian collision, *Geology*, *30*, 263–266.

Dupont-Nivet, G., R. F. Butler, A. Yin, and X. Chen (2003), Paleomagnetism indicates no Neogene vertical axis rotations of the northeastern Tibetan Plateau, *J. Geophys. Res.*, *108*(B8), 2386, doi:10.1029/2003JB002399.

Enkin, R. J., Y. Chen, V. Courtillot, and J. Besse (1991a), A Cretaceous pole from south China, and the Mesozoic hairpin turn of the Eurasian apparent polar wander path, *J. Geophys. Res.*, *96*, 4007–4027.

Enkin, R. J., V. Courtillot, L. Xing, Z. Zhang, Z. Zhuang, and S. Zhang (1991b), The stationary Cretaceous paleomagnetic pole of Sichuan (south China block), *Tectonics*, *10*, 547–559.

Enkin, R. J., Z. Yang, Y. Chen, and V. Courtillot (1992), Paleomagnetic constraints on the geodynamic history of the major blocks of China from the Permian to the Present, *J. Geophys. Res.*, *97*, 13,953–13,989.

Fisher, R. A. (1953), Dispersion on a sphere, *Proc. R. Soc. London, Ser. A*, *217*, 295–305.

Gautam, P., and E. Appel (1994), Magnetic polarity study of Siwlalik Group sediments of Tinau Khola section in west central Nepal, revisited, *Geophys. J. Int.*, *117*, 223–234.

Gautam, P., and Y. Fujiwara (2000), Magnetic polarity stratigraphy of Siwalik Group sediments of Karnail River section in western Nepal, *Geophys. J. Int.*, *142*, 812–824.

Gilder, S., and V. Courtillot (1997), Timing of north-south China collision from new middle to Late Mesozoic paleomagnetic data from the North China Block, *J. Geophys. Res.*, *102*, 17,713–17,727.

Gilder, S. A., R. S. Coe, H. Wu, G. Kuang, X. Zhao, Q. Wu, and X. Tang (1993), Cretaceous and Tertiary paleomagnetic results from southeast China and their tectonic implications, *Earth Planet. Sci. Lett.*, *117*, 637–652.

Gilder, S., J. Gill, R. S. Coe, X. Zhao, Z. Liu, G. Wang, K. Yuan, W. Liu, G. Kuang, and H. Wu (1996), Isotopic and paleomagnetic constraints on the Mesozoic tectonic evolution of South China, *J. Geophys. Res.*, *101*, 16,137–16,154.

Gilder, S., Y. Chen, and S. Sen (2001), Oligo-Miocene magnetostratigraphy and rock magnetism of the Xishuigou section, Subei (Gansu province, western China) and implications for shallow inclinations in central Asia, *J. Geophys. Res.*, *106*, 30,505–30,521.

Gilder, S., Y. Chen, J.-P. Cogné, X. Tan, V. Courtillot, D. Sun, and Y. Li (2003), Paleomagnetism of Upper Jurassic to Lower Cretaceous volcanic and sedimentary rocks from the western Tarim Basin and implications for inclination shallowing and absolute dating of the M-O (ISEA?) chron, *Earth Planet. Sci. Lett.*, *206*, 587–600.

Gorbunov, M. G. (1971), Paleomagnetic directions and pole positions: Data for the USSR, in *World Data Center-B Catalogue*, Issue 1, Sov. Geophys. Comm., Moscow.

Gorshkov, E. S., E. G. Gooskova, V. A. Starunov, T. S. Tyuleneva, Z. Ganhuyach, and P. Khosbayar (1991), Paleomagnetism of western Mongolia, paper presented at IV All-Soviet Union Congress on Geomagnetism, Vladimir-Suzdal, Russia.

Gradstein, F. M., et al. (2004), *A Geologic Time Scale 2004*, 589 pp., Cambridge Univ. Press, New York.

Haag, M., and F. Heller (1991), Late Permian to Early Triassic magnetostratigraphy, *Earth Planet. Sci. Lett.*, *107*, 42–54.

Haihong, C., J. Dobson, F. Heller, and H. Jie (1995), Paleomagnetic evidence for clockwise rotation of the Simao region since the Cretaceous: A consequence of India-Asia collision, *Earth Planet. Sci. Lett.*, *134*, 203–217.

Halim, N., V. Kravchinsky, S. Gilder, J. P. Cogné, M. Alexyutin, A. Sorokin, V. Courtillot, and Y. Chen (1998a), A paleomagnetic study from the Mongol-Okhotsk region: Rotated Early Cretaceous volcanics and remagnetized sediments, *Earth Planet. Sci. Lett.*, *159*, 133–145.

Halim, N., J. P. Cogné, Y. Chen, R. Atasiei, J. Besse, V. Courtillot, S. Gilder, J. Marcoux, and R. L. Zhao (1998b), New Cretaceous and Early Tertiary paleomagnetic results from Xining-Lanzhou basin, Kunlun and Qiangtang blocks, China: Implications on the geodynamic evolution of Asia, *J. Geophys. Res.*, *103*, 21,025–21,045.

Halls, H. C. (1978), The use of converging remagnetization circles in paleomagnetism, *Phys. Earth Planet. Inter.*, *16*, 1–11.

Höck, V., G. Daxner-Hock, H. P. Schmid, D. Badamgarav, W. Frank, G. Furtmüller, O. Montag, R. Barsbold, Y. Khand, and J. Sodov (1999), Oligocene-Miocene sediments, fossils and basalts from the Valley of Lakes (central Mongolia)—An integrated study, *Mitt. Oesterr. Geol. Ges.*, *90*, 83–125.

Huang, K., and N. D. Opdyke (1992), Paleomagnetism of Cretaceous to Lower Tertiary rocks from southwestern Sichuan: A revisit, *Earth Planet. Sci. Lett.*, *112*, 29–40.

Huang, B. C., Y. C. Wang, T. Liu, T. S. Yang, Y. A. Li, D. J. Sun, and R. X. Zhu (2004), Paleomagnetism of Miocene sediments from the Turfan Basin, northwest China: No significant vertical-axis rotation during Neotectonic compression within the Tian Shan Range, central Asia, *Tectonophysics*, *384*, 1–21.

Johnson, D. A., and C. A. Nigrini (1985), Synchronous and time-transgressive Neogene radiolarian datum levels in the equatorial Indian and Pacific Oceans, *Mar. Micropaleontol.*, *9*, 489–523.

Kent, D. V., V. Xu, K. Huang, W. Zhang, and N. D. Opdyke (1987), Paleomagnetism of Upper Cretaceous rocks from south China, *Earth Planet. Sci. Lett.*, *139*, 133–143.

Kepezhinskas, V. V. (1979), Cenozoic alkaline basaltoids of Mongolia and related deep inclusions, report, 311 pp., Jt. Sov.-Mongol. Sci. Res. Geol. Exped., Moscow.

Khramov, A. N. (1970), Generalized paleomagnetic section for the Mesozoic of the southern Tajikistan, *Materialy 8 konf po postoyan polyu i paleomagn*, pp. 235–238.

Khramov, A. N. and I. P. Slautsitais (1982), Paleomagnetic directions and pole positions: Data for the USSR, in *World Data Center-B Catalogue*, Issue 5, *Sov. Geophys. Comm.*, Moscow.

Kikawa, E., R. McCabe, J. Han, K. D. Min, D. Lee, H.-C. Han, and J. A. Hwang (1994), Miocene paleomagnetic results from southeastern Korea, *Tectonophysics*, *233*, 115–123.

Kirshvink, J. L. (1980), The least-squares line and plane and the analysis of paleomagnetic data, *Geophys. J. R. Astron. Soc.*, *60*, 699–718, 1980.

Klootwijk, C. T., M. L. Sharma, J. Gergan, B. Tirkey, S. K. Shah, and V. Agarwal (1979), The extent of greater India, II. Paleomagnetic data from the Ladakh intrusives at Kargil, northwestern Himalayas, *Earth Planet. Sci. Lett.*, *44*, 47–64.

Klootwijk, C. T., R. Nazirullah, K. A. De Jong, and H. Ahmed (1981), A paleomagnetic reconnaissance of northeastern Baluchistan, Pakistan, *J. Geophys. Res.*, *86*, 289–306.

Klootwijk, C. T., A. K. Jain, and R. Khorana (1982), Palaeomagnetic constraints on allochthony and age of the Krol Belt sequence, Garhwal Himalaya, India, *J. Geophys.*, *50*, 127–136.

Klootwijk, C. T., M. L. Sharma, J. Gergan, S. K. Shah, and B. K. Gupta (1986), Rotational overthrusting of the northwestern Himalaya: Further palaeomagnetic evidence from the Riasi thrust sheet, Jammu foothills, India, *Earth Planet. Sci. Lett.*, *80*, 375–393.

Kovalenko, D. V., V. V. Yarmolyuk, and A. V. Solov'ev (1997), Migration of volcanic centers of the south Khangai hot spot: Paleomagnetic evidence, *Geotectonics*, *31*, 228–235.

Kravchinsky, V. A., J. P. Cogné, W. Harbert, and M. I. Kuzmin (2002), Evolution of the Mongol-Okhotsk ocean as constrained by new paleomagnetic data from the Mongol-Okhotsk suture zone, *Geophys. J. Int.*, *148*, 34–57.

Krumsiek, K. (1976), Zur bewegung Iranisch-Afghanischen platte (palaomagnetische ergebnisse), *Geol. Rundsch.*, *65*, 909–929.

Lee, G., J. Besse, and V. Courtillot (1987), Eastern Asia in the Cretaceous: New paleomagnetic data from South Korea and new look at the Chinese and Japanese data, *J. Geophys. Res.*, *92*, 3580–3596.

Lee, Y. S., N. Ishikawa, and W. K. Kim (1999), Paleomagnetism of Tertiary rocks on the Korean Peninsula: Tectonic implications for the opening of the East Sea (Sea of Japan), *Tectonophysics*, *304*, 131–149.

Le Goff, M. (1990), Lissage et limites d'incertitude des courbes de migration polaire; pondération des données et extension bivariate de la statistique de Fisher, *C. R. Acad. Sci., Ser. II*, *311*, 1191–1198.

Liu, Z., X. Zhao, C. Wang, S. Liu, and H. Yi (2003), Magnetostratigraphy of Tertiary sediments from the Hoh Xil Basin: Implications for the Cenozoic tectonic history of the Tibetan Plateau, *Geophys. J. Int.*, *154*, 233–252.

Ma, X., Z. Yang, and L. Xing (1993), The Lower Cretaceous reference pole for north China, and its tectonic implications, *Geophys. J. Int.*, *115*, 323–331.

Mammedov, M. (1971), Paleomagnetic directions and pole positions: Data for the USSR, in *World Data Center-B Catalogue*, Issue 1, *Sov. Geophys. Comm.*, Moscow.

McElhinny, M. W., and J. Lock (1996), IAGA paleomagnetic data bases with access, *Surv. Geophys.*, *17*, 575–591.

McFadden, P. L., and F. J. Lowes (1981), The discrimination of mean directions drawn from Fisher distributions, *Geophys. J. R. Astron. Soc.*, *67*, 19–33.

McFadden, P. L., and M. W. McElhinny (1988), The combined analysis of remagnetization circles and direct observations in paleomagnetism, *Earth Planet. Sci. Lett.*, *87*, 161–172.

McFadden, P. L., R. T. Merill, M. W. McElhinny, and L. Sunhee (1991), Reversal of the Earth's magnetic field and temporal variations of the dynamo families, *J. Geophys. Res.*, *96*, 3923–3933.

Molnar, P., and P. Tapponnier (1975), Cenozoic tectonics of Asia: Effects of a continental collision, *Science*, *189*, 419–426.

Morinaga, H., and Y. Liu (2004), Cretaceous paleomagnetism of the eastern South China Block: Establishment of the stable body of SCB, *Earth Planet. Sci. Lett.*, *222*, 971–988.

Narumoto, K., Z. Yang, K. Takemoto, H. Zaman, H. Morinaga, and Y. I. Otofuji (2006), Anomalously shallow inclination in middle–northern part of the South China block: Palaeomagnetic study of Late Cretaceous red beds from Yichang area, *Geophys. J. Int.*, *164*, 290–300.

Ojha, T. P., R. F. Butler, J. Quade, P. G. DeCelles, D. Richards, and B. N. Upreti (2000), Magnetic polarity stratigraphy of the Neogene Siwalik Group at Khutia Khola, far western Nepal, *Geol. Soc. Am. Bull.*, *112*, 424–434.

Opdyke, N. D., N. M. Johnson, G. D. Johnson, E. H. Lindsay, and R. A. K. Tahirkheli (1982), Paleomagnetism of the Middle Siwalik Formations of Northern Pakistan and rotation of the Salt Range decollement, *Paleogeogr. Paleoclimatol. Paleoecol.*, *37*, 1–15.

Otofuji, Y. I., et al. (1995), Late Cretaceous to early Paleogene paleomagnetic results from Sikhote Alin, far eastern Russia: Implications for deformation of east Asia, *Earth Planet. Sci. Lett.*, *130*, 95–108.

Otofuji, Y. I., et al. (2003), Late Cretaceous paleomagnetic results from Sikhote Alin, far eastern Russia: Tectonic implications for the eastern margin of the Mongolia Block, *Geophys. J. Int.*, *152*, 202–214.

Pruner, P. (1992), Paleomagnetism and paleogeography of Mongolia from the Carboniferous to Cretaceous—Final report, *Phys. Earth Planet. Inter.*, *70*, 169–177.

Puchkov, V. N. (1997), Structure and geodynamics of Uralian orogen, in *Orogeny Through Time*, edited by J.-P. Burg and M. Ford, *Geol. Soc. Spec. Publ.*, *121*, 201–236.

Quidelleur, X., J. P. Valet, V. Courtillot, and G. Hulot (1994), Long-term geometry of the geomagnetic field for the last five million years: An updated secular variation database, *Geophys. Res. Lett.*, *21*(15), 1639–1642.

Rasskazov, S. V., N. A. Logatchev, I. S. Brandt, S. B. Brandt, and A. V. Ivanov (2000), *Geochronology and Geodynamics in the Late Cenozoic: South Siberia-South and East Asia*, 288 pp., Nauka, Novosibirsk, Russia.

Si, J., and R. Van der Voo (2001), Too-low magnetic inclinations in central Asia: An indication of long-term Tertiary non-dipole field?, *Terra Nova*, *13*, 471–478.

Sun, Z., Z. Yang, J. Pei, T. Yang, and X. Wang (2006a), New Early Cretaceous paleomagnetic data from volcanic and red beds of the eastern Qaidam Block and its implications for tectonics of central Asia, *Earth Planet. Sci. Lett.*, *243*, 268–281.

Sun, Z., Z. Yang, T. Yang, J. Pei, and Q. Yu (2006b), New Late Cretaceous and Paleogene paleomagnetic results from south China and their geodynamic implications, *J. Geophys. Res.*, *111*, B03101, doi:10.1029/2004JB003455.

Tan, X., K. P. Kodama, H. Chen, D. Fang, D. Sun, and Y. Li (2003), Paleomagnetism and magnetic anisotropy of Cretaceous red beds from the Tarim basin, northwest China: Evidence for a rock magnetic cause of anomalously shallow paleomagnetic inclinations from central Asia, *J. Geophys. Res.*, *108*(B2), 2107, doi:10.1029/2001JB001608.

Tapponnier, P., and P. Molnar (1979), Active faulting and Cenozoic tectonics of Tien Shan, Mongolia, and Baykal regions, *J. Geophys. Res.*, *84*, 3425–3459.

Tapponnier, P., G. Peltzer, and R. Armijo (1986), On the mechanics of the collision between India and Asia, in *Collision Tectonics*, edited by M. P. Coward and A. C. Ries, *Geol. Soc. Spec. Publ.*, *19*, 115–157.

Tauxe, L. (2005), Inclination flattening and the geocentric axial dipole hypothesis, *Earth Planet. Sci. Lett.*, *233*, 247–261.

Thomas, J.-C., H. Perroud, P. R. Cobbold, M. L. Bazhenov, V. S. Burtman, A. Chauvin, and E. Sadybakasov (1993), A paleomagnetic study of tertiary formations from the Kyrgyz Tien-Shan and its tectonic implications, *J. Geophys. Res.*, *98*, 9571–9590.

Thomas, J. C., A. Chauvin, D. Gapais, M. L. Bazhenov, H. Perroud, P. R. Cobbold, and V. S. Burtman (1994), Paleomagnetic evidence for Cenozoic block rotations in the Tadjik depression (central Asia), *J. Geophys. Res.*, *99*, 15,141–15,160.

Torcq, F. (1997), Evolution et destruction de la Pangée du Carbonifère au Jurassique, dérive des pôles magnétiques et étude de la dipolarité du champ, thesis, 183 pp., Univ. Paris 7, Paris.

Torsvik, T. H., and R. Van der Voo (2002), Refining Gondwana and Pangea palaeogeography: Estimates of Phanerozoic non-dipole (octupole) fields, *Geophys. J. Int.*, *151*, 771–794.

Van der Voo, R., and T. H. Torsvik (2001), Evidence for late Paleozoic and Mesozoic non-dipole fields provides an explanation for the Pangea reconstruction problems, *Earth Planet. Sci. Lett.*, *187*, 71–81.

Wensink, H. (1972), A note on the Paleomagnetism of the Lower Siwaliks near Choa Saiden Shah, Potwar Plateau, West Pakistan, Pakistan, *J. Sci. Ind. Res.*, *15*, 89–91.

Westphal, M. (1993), Did a large departure from the geocentric axial dipole occur during the Eocene? Evidence from the magnetic polar wander path of Eurasia, *Earth Planet. Sci. Lett.*, *117*, 15–28.

Whitford-Stark, J. L. (1987), A survey of Cenozoic volcanism on mainland Asia, *Spec. Pap. Geol. Soc. Am.*, *213*, 20–23.

Windley, B. F., and M. B. Allen (1993), Mongolian plateau: Evidence for a late Cenozoic mantle plume under central Asia, *Geology*, *21*, 295–298.

Yang, T., Z. Yang, Z. Sun, and A. Li (2001), New Early Cretaceous paleomagnetic results from the Qilian orogenic belt and its tectonic implications, *Sci. China*, *44*, 568–576.

Yang, Z., and J. Besse (1993), Paleomagnetic study of Permian and mesozoic sedimentary rocks from northern Thailand supports the extrusion model for Indochina, *Earth Planet. Sci. Lett.*, *117*, 525–552.

Yang, Z., and J. Besse (2001), New Mesozoic apparent polar wander path for south China: Tectonic consequences, *J. Geophys. Res.*, *106*, 8493–8520.

Yarmolyuk, V. V., V. G. Ivanov, V. S. Samoylov, and M. M. Arakelyants (1995), Formation stages of Mesosoic and Cenozoic intraplate volcanism of south Mongolia (in Russian), *Dokl. Acad. Nauk*, *344*(5), 673–676.

Yeroshkin, A. F. (1973), Paleomagnetic directions and pole positions: Data for the USSR, in *World Data Center-B Catalogue*, Issue 2, *Sov. Geophys. Comm.*, Moscow.

Yeroshkin, A. F. (1982), Paleomagnetic directions and pole positions: Data for the USSR, in *World Data Center-B Catalogue*, Issue 5, *Sov. Geophys. Comm.*, Moscow.

Zhao, X. (1987), A paleomagnetic study of Phanerozoic rock units from eastern China, Ph.D. thesis, 402 pp., Univ. of Calif., Santa Cruz.

Zhao, X., and R. S. Coe (1987), Paleomagnetic constraints on the collision and rotation of north and south China, *Nature*, *327*, 141–144.

Zhao, X., R. S. Coe, Y. Zhou, H. Wu, and J. Wang (1990), New paleomagnetic results from northern China: Collision and suturing with Siberia and Kazakstan, *Tectonophysics*, *181*, 43–81.

Zhao, X., R. S. Coe, Y. Zhou, S. Hu, H. Wu, G. Kuang, Z. Dong, and J. Wang (1994), Tertiary paleomagnetism of north and south China and a reappraisal of Late Mesozoic paleomagnetic data from Eurasia: Implications for the Cenozoic tectonic history of Asia, *Tectonophysics*, *235*, 181–203.

Zheng, Z., M. Kono, H. Tsunakawa, G. Kimura, Q. Wei, X. Zhu, and T. Hao (1991), The apparent polar wander path for the North China Block since the Jurassic, *Geophys. J. Int.*, *104*, 29–40.

Zhu, Z., and T. Hao (1988), Paleomagnetic study on the tectonic motion of Pan-Xi block and adjacent area during Yin Zhi-Yanshan period (in Chinese), *Acta Geophys. Sin.*, *31*, 420–431.

Zijderveld, J. D. A. (1967), A. C. demagnetization of rocks: Analysis of results, in *Methods in Paleomagnetism*, edited by D. W. Collinson, K. M. Creer, and S. K. Runcorn, pp. 254–286, Elsevier, New York.

A. Bayasgalan and P. Lkhagvadorj, School of Geology, Mongolian University of Science and Technology, P.O. Box 49/418, Ulaanbaatar 210349, Mongolia.

L. Carporzen, J.-P. Cogné, and F. Hankard, Laboratoire de Paléomagnétisme, Institut de Physique du Globe de Paris et Université Paris 7, 4 Place Jussieu, F-75252 Paris Cedex 05, France. (hankard@ipgp.jussieu.fr)

V. A. Kravchinsky, Physics Department, University of Alberta, Edmonton, AB, Canada T6G 2J1.